Article:

Palamara, Antonio, Plastina, Francesco, Sindona, Antonello et al. (1 more author) (2024) Thermal-density-functional-theory approach to quantum thermodynamics. Physical Review A. 062203. ISSN 1094-1622

https://doi.org/10.1103/PhysRevA.110.062203

PHYSICAL REVIEW A **110**, 062203 (2024)

Thermal-density-functional-theory approach to quantum thermodynamics

Antonio Palamara,[1,2] Francesco Plastina,[1,2] Antonello Sindona,[1,2] and Irene D'Amico[3,*]
[1]*Dipartimento di Fisica, Università della Calabria, Via P. Bucci, Cubo 30C, I-87036 Rende (CS), Italy*
[2]*INFN, sezione LNF, Gruppo collegato di Cosenza, Via P. Bucci, Cubo 31C, I-87036 Rende (CS), Italy*
[3]*School of Physics, Engineering and Technology, The University of York, York YO10 5DD, United Kingdom*

(Received 5 September 2024; accepted 18 November 2024; published 2 December 2024)

Understanding the thermodynamic properties of many-body quantum systems and their emergence from microscopic laws is a topic of great significance due to its profound fundamental implications and extensive practical applications. Recent advances in experimental techniques for controlling and preparing these systems have increased interest in this area, as they have the potential to drive the development of quantum technologies. In this study, we present a density-functional-theory approach to extract detailed information about the statistics of work and the irreversible entropy associated with quantum quenches at finite temperature. Specifically, we demonstrate that these quantities can be expressed as functionals of thermal and out-of-equilibrium densities, which may serve as fundamental variables for understanding finite-temperature many-body processes. We, then, apply our method to the case of the inhomogeneous Hubbard model, showing that our density-functional-theory-based approach can be usefully employed to unveil the distinctive roles of interaction and external potential on the thermodynamic properties of such a system.

DOI: 10.1103/PhysRevA.110.062203

I. INTRODUCTION

Density-functional theory (DFT) [1,2] and its time-dependent (TD) extension [3,4] are powerful and well-established methods for studying the electronic properties of interacting many-body systems at zero temperature, with DFT providing comprehensive access to ground-state properties and TDDFT extending this capability to include the prediction of excited states. Thermal-density-functional theory (ThDFT), introduced by Mermin [5], extends the Hohenberg-Kohn (HK) framework of DFT [1] to address the electronic properties of many-body systems under conditions where accounting for finite-temperature effects is indispensable [6–15].

Renewed attention in ThDFT has been driven by the study of thermal properties of out-of-equilibrium interacting quantum systems, which represents a major focus in quantum thermodynamics (QT). This field is rapidly evolving thanks to advances in preparing and coherently controlling quantum systems at the microscopic scale, enabling experimental verification of fundamental properties such as fluctuation theorems [16–19]. These developments also hold potential for new quantum technologies based on complex quantum systems (see, e.g., [20]). A major goal in QT is to understand the role of purely quantum features, such as coherence and correlations, in thermodynamic processes. This notably includes work processes, where work is extracted from or performed on a quantum system, and the generation of irreversible entropy [21–38].

In this realm, the emphasis is rapidly shifting towards coupled many-body systems (see, e.g, [39,40]). Indeed, recent studies have demonstrated that particle interactions can enhance the efficiency of quantum heat engines [34,41–44]. On the theoretical side, addressing finite-temperature quantum many-body systems poses significant challenges, often requiring approximations to manage their complexity.

In this context, and drawing inspiration from previous works [45–48], our objective is to establish a robust theoretical framework for applying DFT to the study of nonequilibrium thermodynamics in quenched interacting many-body systems. Our formalism focuses on the canonical ensemble, of particular relevance for QT thermal machines. Specifically, we demonstrate that the thermal and out-of-equilibrium densities form the basis of an *ab initio* framework for deriving thermodynamic properties of quantum systems that experience a sudden quench. A key advantage is that the out-of-equilibrium thermodynamics of interacting many-body systems can be effectively investigated using the Kohn-Sham (KS) approach to DFT [2]. The strength of this approach lies in its ability to evaluate, in principle exactly, the thermal densities by mapping the original interacting many-body system onto a fictitious noninteracting one. We thus establish a general framework for the DFT approach to QT, specifically for the canonical ensemble, and validate it through the analysis of the quenched inhomogeneous Hubbard model. Accordingly, we first compare results from exact diagonalization for small systems with those obtained using our finite-temperature KS mapping, and then extend our analysis to larger systems. This extension allows us to clarify how interactions influence thermal densities and, consequently, the work performed.

---

[*] Contact author: irene.damico@york.ac.uk

The remainder of the paper is organized as follows. In Sec. II, we recall the Mermin-Hohenberg-Kohn (MHK) theorem [1,5], adapting it to the context of lattice Hamiltonians in closed quantum systems. In Sec. III, we review the fundamental concepts of out-of-equilibrium QT, showing that for work protocols of infinitesimal duration, the probability distributions of work and irreversible entropy production are completely determined by the finite-temperature equilibrium densities of the prequench and postquench Hamiltonians. In Sec. IV, we recall the Mermin-Kohn-Sham (MKS) equations [2,5], employing the finite-temperature KS mapping to calculate the thermodynamic quantities of interest. In Sec. V, we present a method for calculating the thermal densities of a system of indistinguishable particles within the canonical ensemble using the KS mapping. In Sec. VI, we apply our theoretical framework to short Hubbard chains, solving the problem both exactly and via the finite-temperature KS mapping to validate the robustness and accuracy of our DFT-based approach. We then extend our DFT-based analysis to the Hubbard model with a larger number of sites. Finally, we draw our conclusions in Sec. VII.

II. THERMAL {A}-FUNCTIONAL THEORY

In its original formulation, DFT is founded on the HK theorems [1], which were later generalized to finite temperatures by Mermin [5]. These theorems establish a one-to-one correspondence between the external potential $v(\mathbf{r})$ [or $v(\mathbf{r})-\mu$, where μ is the chemical potential], the quantum (equilibrium) state of the system, and the ground-state (or thermal) electron density $n(\mathbf{r})$ [or $n^{\beta}(\mathbf{r})$]. More recently, it has been demonstrated that the HK theorems at zero temperature are still valid for quantum systems whose Hamiltonian is defined on a lattice [49–51], with some limitations [52–54]. Similarly, it can be shown that this extension also holds true for finite-temperature closed quantum systems.

To demonstrate this, let us consider a closed quantum system governed by a Hamiltonian $\hat{\mathcal{H}}$ of the following form:

$$\hat{\mathcal{H}}[\{\lambda_i\}] = \hat{\mathcal{H}}_0 + \hat{\mathcal{V}}_{\text{EXT}}[\{\lambda_i\}] = \hat{\mathcal{H}}_0 + \sum_{i=1}^{\mathcal{L}} \lambda_i \hat{A}_i, \tag{1}$$

where $\hat{\mathcal{H}}$ is quite general and can describe spin chains, fermionic, or bosonic systems. $\hat{\mathcal{H}}_0$ is the "*universal*" HK Hamiltonian, and $\hat{\mathcal{V}}_{\text{EXT}}$ is the external potential, controlled by a set of $\mathcal{L}$ parameters $\{\lambda_i\}$ that multiply the local operators $\{\hat{A}_i\}$.

Let us denote the thermal expectation value of $\hat{A}_i$ as

$$a_i^{\beta} := \text{Tr}\{\hat{\rho}_{\beta}^{\text{TH}}[\{\lambda_i\}]\hat{A}_i\}, \tag{2}$$

where $\hat{\rho}_{\beta}^{\text{TH}}[\{\lambda_i\}] = e^{-\beta\hat{\mathcal{H}}[\{\lambda_i\}]}/\mathcal{Z}[\{\lambda_i\}]$ represents the Gibbs state and $\mathcal{Z}[\{\lambda_i\}] = \text{Tr}\{e^{-\beta\hat{\mathcal{H}}[\{\lambda_i\}]}\}$ expresses the canonical partition function. By definition, each a_i^{β} is a function of the parameters $\{\lambda_i\}$. It can be shown that exactly one parameter set $\{\lambda_i\}$ corresponds to a given mean value set $\{a_i^{\beta}\}$ (see Appendix A).

Since $\{a_i^{\beta}\}$ uniquely determines $\{\lambda_i\}$, which in turn determines $\hat{\rho}_{\beta}^{\text{TH}}$, the thermal state is also a unique functional of $\{a_i^{\beta}\}$. This relationship highlights the direct connection between observable mean values and the underlying thermal state, emphasizing the role of $\{a_i^{\beta}\}$ as the fundamental descriptors of the system:

$$\{\lambda_i\} \iff \{a_i^{\beta}\} \iff \hat{\rho}_{\beta}^{\text{TH}} \equiv \hat{\rho}_{\beta}^{\text{TH}}[\{a_i^{\beta}\}]. \tag{3}$$

By the one-to-one relations established in Eq. (3), the thermal HK theorem, as demonstrated by Mermin [5], remains valid for closed quantum systems defined by the Hamiltonian (1). Consequently, the free energy

$$\mathcal{F}[\hat{\rho}] := \text{Tr}\left\{\hat{\rho}\left(\hat{\mathcal{H}} + \frac{\ln\hat{\rho}}{\beta}\right)\right\}, \tag{4}$$

minimized by the equilibrium Gibbs state, can be expressed as a unique function of $\{\lambda_i\}$ or, equivalently, as a unique functional of $\{a_i^{\beta}\}$:

$$\mathcal{F}[\{a_i^{\beta}\}] = \Omega[\{a_i^{\beta}\}] + \sum_{i=1}^{\mathcal{L}} \lambda_i a_i^{\beta}. \tag{5}$$

Here, $\Omega[\{a_i^{\beta}\}]$ represents the generally unknown "*universal*" functional [55], associated with the $\{\lambda_i\}$-independent Hamiltonian $\hat{\mathcal{H}}_0$. Similarly to the zero-temperature case [49,50], Eq. (5) allows us to interpret the HK theorem as an expression of duality in the sense of a Legendre transform. This duality relates the thermal expectation values $\{a_i^{\beta}\}$, which play a role analogous to the thermal electron densities $n^{\beta}(\mathbf{r})$, to the set of work parameters $\{\lambda_i\}$, which fulfill a role analogous to the external potentials $v(\mathbf{r})$.

A special case of the Hamiltonian (1) corresponds to the following single-parameter scenario:

$$\hat{\mathcal{H}}[\lambda] = \hat{\mathcal{H}}_0 + \lambda\sum_{i=1}^{\mathcal{L}} \hat{A}_i, \tag{6}$$

where the HK theorem remains valid. However, to ensure a unique mapping between λ and

$$\langle\hat{A}\rangle \equiv \text{Tr}\left\{\hat{\rho}_{\beta}^{\text{TH}}[\{\lambda_i\}]\sum_{i=1}^{\mathcal{L}} \hat{A}_i\right\}, \tag{7}$$

it is necessary to require that $[\hat{\mathcal{H}}_0, \sum_{i=1}^{\mathcal{L}} \hat{A}_i] \neq 0$ [56].

Another important tool is offered by the Hellmann-Feynman (HF) theorem [49,57,58], which establishes a relationship between the first derivative of the free energy with respect to the ith external parameter and the ith thermal density:

$$\frac{\partial\mathcal{F}}{\partial\lambda_i} = \text{Tr}\left\{\hat{\rho}_{\beta}^{\text{TH}}[\{\lambda_i\}]\frac{\partial\hat{\mathcal{H}}}{\partial\lambda_i}\right\} = \text{Tr}\{\hat{\rho}_{\beta}^{\text{TH}}[\{\lambda_i\}]\hat{A}_i\} = a_i^{\beta}. \tag{8}$$

This equation will be especially useful in the subsequent sections, particularly in the context of thermal sudden quenches, where thermal expectation values serve as fundamental variables for deriving the thermodynamic quantities of interest.

III. THERMAL {A}-FUNCTIONAL THEORY APPROACH TO QUANTUM THERMODYNAMICS

ThDFT can be effectively employed to extract information about the out-of-equilibrium thermodynamics of a closed quantum system by leveraging its ability to handle thermal and quantum fluctuations. To establish the formalism, we first review some key concepts in QT. Our focus is on a closed quantum system that has been driven out of equilibrium by a unitary quantum process. Specifically, we consider a generic closed quantum system characterized by the Hamiltonian (1), which depends on a set of time-dependent work parameters $\{\lambda_i^t\}$. The system is initially in equilibrium with a bath at inverse temperature β. In this configuration, at $t = 0$, the set of work parameters $\{\lambda_i^0\}$ defines the thermal state, represented by the Gibbs density operator $\hat{\rho}_\beta^{\text{TH}}[\{\lambda_i^0\}]$. After the system is decoupled from the bath, it undergoes unitary dynamics, from $t = 0$ to τ, governed by the time-evolution operator $\hat{\mathcal{U}}(\tau, 0)$. This evolution is driven by a protocol that changes the set of work parameters from $\{\lambda_i^0\}$, with corresponding mean values $\{a_i^{\beta\,0}\}$, to $\{\lambda_i^f\}$, with corresponding mean values $\{a_i^{\beta\,f}\}$, over the finite-time interval τ.

A. Probability distributions of work and irreversible entropy production

The work performed or extracted during the protocol is not an observable and cannot be represented by a Hermitian operator. Rather, work is a stochastic variable characterized by a probability distribution, which is determined by performing two projective measurements at the initial and final times, respectively [59–61].

This "two-point measurement" scheme, while potentially problematic for states with initial coherence in the energy basis (see Refs. [31,62–65]), is well suited for describing work statistics in the case of initial thermal states, which we will assume in the following analysis.

These two measurements involve the instantaneous eigenbasis of the system Hamiltonian denoted $\{\epsilon_n(t), |n(t)\rangle\}$. The probability distribution of work (PDW) is defined as follows:

$$P_\tau(w) = \sum_{nm} p_n(0) p_{n\to m}(\tau)\delta(w - w_{mn}), \tag{9}$$

where $w_{mn} = \epsilon_m(\tau) - \epsilon_n(0)$ is the work performed in a single realization, $p_n(0) \equiv \langle n(0)|\hat{\rho}_\beta^{\text{TH}}|n(0)\rangle$ is the probability of finding the system in the nth eigenstate at time $t = 0$, and $p_{m\to n}(\tau)$ is the transition probability, between the nth and mth eigenstates, due to the protocol. Fluctuations arising from the protocol and the measurements are encoded by $p_n(0)p_{m\to n}(\tau)$ and constrained by the Jarzynski's equality [16]

$$\langle e^{-\beta w}\rangle = e^{-\beta\Delta\mathcal{F}}, \tag{10}$$

where $\Delta\mathcal{F} = \mathcal{F}[\{\lambda_i^f\}] - \mathcal{F}[\{\lambda_i^0\}]$ is the free-energy difference between the two equilibrium configurations, corresponding to the initial and final Hamiltonians.

By the Jensen's inequality, Eq. (10) implies that $\langle w\rangle \geqslant \Delta\mathcal{F}$, which reflects the second law of thermodynamics. This leads to the definition of the average irreversible work [66]

$$\langle w_{\text{IRR}}\rangle := \langle w\rangle - \Delta\mathcal{F}, \tag{11}$$

which is directly related to the average irreversible entropy production [61,67,68]

$$\langle \mathcal{S}_{\text{IRR}}\rangle := \beta\langle w_{\text{IRR}}\rangle. \tag{12}$$

Both $\langle w_{\text{IRR}}\rangle$ and $\langle \mathcal{S}_{\text{IRR}}\rangle$ give a measure of the irreversibility introduced by performing the unitary transformation $\hat{\rho}(\tau) = \hat{\mathcal{U}}(\tau, 0)\hat{\rho}_\beta^{\text{TH}}[\{\lambda_i^0\}]\hat{\mathcal{U}}^\dagger(\tau, 0)$. Strictly speaking, due to the unitary nature of the time evolution, no von Neumann entropy is generated during this process, with the entropy of the system remaining constant:

$$\mathcal{S}[\hat{\rho}(\tau)] = -\text{Tr}\{\hat{\rho}(\tau)\log\hat{\rho}(\tau)\} \equiv \mathcal{S}\big(\hat{\rho}_\beta^{\text{TH}}\big[\{\lambda_i^0\}\big]\big). \tag{13}$$

Equation (12) is referred to as a measure of irreversibility because, when the system is returned to the bath after the protocol, it relaxes from the out-of-equilibrium state to the thermal state $\hat{\rho}_\beta^{\text{TH}}[\{\lambda_i^f\}]$. This relaxation is a nonunitary process, and the entropy produced during this process is precisely $\langle \mathcal{S}_{\text{IRR}}\rangle$.

We emphasize that, like the average work, $\langle \mathcal{S}_{\text{IRR}}\rangle$ is also the first moment of a probability distribution obtained within the two-point measurement framework. Indeed, it is possible to define a stochastic variable, associated with the production of irreversible entropy, as follows:

$$s_{mn} := \beta[\epsilon_m(\tau) - \epsilon_n(0)] - \beta\Delta\mathcal{F}. \tag{14}$$

Then, the probability distribution for entropy production (PDEP), analogous to the PDW, takes the form

$$P_\tau(s) = \sum_{nm} p_n(0)p_{n\to m}(\tau)\delta(s - s_{mn}). \tag{15}$$

A complementary approach to investigate the statistical properties of work processes and irreversible entropy production is based on the Fourier transforms of the corresponding probability distributions, namely, $P_\tau(w)$ from Eq. (9) and $P_\tau(s)$ from Eq. (15). It is therefore convenient to rely on the characteristic function of work [61]

$$\begin{aligned}\chi_\nu(w,\tau) &:= \int dw\, e^{i\nu w}P_\tau(w)\\ &= \text{Tr}\big\{e^{i\nu\hat{\mathcal{H}}[\{\lambda_i^f\}]}\mathcal{U}(\tau,0)e^{-i\nu\hat{\mathcal{H}}[\{\lambda_i^0\}]}\\ &\quad\times\hat{\rho}_\beta^{\text{TH}}\big(\big[\{\lambda_i^0\}\big]\big)\mathcal{U}^\dagger(\tau,0)\big\},\end{aligned} \tag{16}$$

with associated moments

$$\langle w^n(\tau)\rangle = (-i)^n\partial_\nu^n\chi_\nu(w,\tau)|_{\nu=0}. \tag{17}$$

It is further instructive to introduce the characteristic function for irreversible entropy production:

$$\begin{aligned}\chi_\mu(s,\tau) &:= \int ds\, e^{i\mu s}P_\tau(s)\\ &= e^{-i\beta\mu\Delta\mathcal{F}}\text{Tr}\big\{e^{i\beta\mu\hat{\mathcal{H}}[\{\lambda_i^f\}]}\hat{\mathcal{U}}(\tau,0)\\ &\quad\times e^{-i\beta\mu\hat{\mathcal{H}}[\{\lambda_i^0\}]}\hat{\rho}_\beta^{\text{TH}}\big[\{\lambda_i^0\}\big]\hat{\mathcal{U}}^\dagger(\tau,0)\big\},\end{aligned} \tag{18}$$

with associated moments

$$\langle s^n(\tau)\rangle = (-i)^n\partial_\mu^n\chi_s(w,\tau)|_{\mu=0}. \tag{19}$$

The two quantities expressed in Eqs. (16) and (18) play a crucial role in the development of the thermal-density-functional framework for specific protocols, as detailed in Sec. III B (sudden quench) and Appendix B (finite-time protocols).

B. Sudden-quench protocol

A sudden quench involves an instantaneous shift of the work parameters, from $\{\lambda_i^0\}$ to $\{\lambda_i^f\}$. This variation occurs in an infinitesimally short timeframe, unlike the finite-time protocols covered in Appendix B. It can be demonstrated that all of the moments of the PDW in this scenario are functionals of the initial thermal densities. This outcome is due to the fact that, in a sudden quench, the time-evolution operator approaches the identity operator, as the quench duration becomes infinitesimally small [69]: $\lim_{\tau\to 0^+}\hat{\mathcal{U}}(\tau,0)=\hat{1}$. Therefore, the characteristic function of work (16) simplifies to an ensemble average over the initial Gibbs state:

$$\chi_\nu(w,0^+)=\mathrm{Tr}\big\{e^{i\nu\hat{\mathcal{H}}[\{\lambda_i^f\}]}e^{-i\nu\hat{\mathcal{H}}[\{\lambda_i^0\}]}\hat{\rho}_\beta^{\mathrm{TH}}\big[\{\lambda_i^0\}\big]\big\}. \tag{20}$$

For a Hamiltonian of the form (1), any thermal average over the initial state can be expressed as a functional of the initial mean values $\{a_i^{\beta\,0}\}$, as dictated by the generalized HK theorem outlined in Sec. II and Appendix A. Consequently, we have $\chi_\nu(w,0^+)=\chi_\nu(w,0^+)[\{a_i^{\beta\,0}\}]$, which implies that all the moments of $P_{0^+}(w)$ are functionals of $\{a_i^{\beta\,0}\}$, with parametric dependence on both $\{\lambda_i^0\}$ and $\{\lambda_i^f\}$. More explicitly, by using Eq. (17), these moments can be expressed as the following thermal averages:

$$\langle w^n\rangle=\mathrm{Tr}\big\{\big(\hat{\mathcal{H}}\big[\{\lambda_i^f\}\big]-\hat{\mathcal{H}}\big[\{\lambda_i^0\}\big]\big)^n\hat{\rho}_\beta^{\mathrm{TH}}\big[\{\lambda_i^0\}\big]\big\}, \tag{21}$$

which are functional of the initial thermal densities: $\langle w^n\rangle=\langle w^n\rangle[\{a_i^{\beta\,0}\}]$. Now, the linearity of the Hamiltonian $\mathcal{H}[\{\lambda_i\}]$ in the work parameters $\{\lambda_i\}$ leads to

$$\hat{\mathcal{H}}\big[\{\lambda_i^f\}\big]-\hat{\mathcal{H}}\big[\{\lambda_i^0\}\big]=\sum_i\big(\lambda_i^f-\lambda_i^0\big)\frac{\partial\hat{\mathcal{H}}}{\partial\lambda_i^0}. \tag{22}$$

Then, using Eqs. (21) and (22), the average work becomes

$$\langle w\rangle=\sum_i\big(\lambda_i^f-\lambda_i^0\big)a_i^{\beta\,0}. \tag{23}$$

Similarly, the characteristic function of the irreversible entropy production (15), for a sudden-quench protocol, takes the simplified expression

$$\begin{aligned}\chi_\mu(s,0^+)=&\,e^{-i\beta\mu\Delta\mathcal{F}}\mathrm{Tr}\big\{e^{i\beta\mu\hat{\mathcal{H}}[\{\lambda_i^f\}]}\\&\times e^{-i\beta\mu\hat{\mathcal{H}}[\{\lambda_i^0\}]}\hat{\rho}_\beta^{\mathrm{TH}}\big[\{\lambda_i^0\}\big]\big\}.\end{aligned} \tag{24}$$

Again, by virtue of the thermal HK theorem, the final and initial free energies in $\Delta\mathcal{F}$ are functionals of $\{a_i^{\beta\,f}\}$ and $\{a_i^{\beta\,0}\}$, respectively. On the other hand, as seen in Eq. (20), the trace in Eq. (24) is a functional of $\{a_i^{\beta\,0}\}$ only. Consequently, we can assert that $P_{0^+}(s)$, or $\chi_\mu(s,0^+)$, and the associated moments $\langle s^n\rangle$ are functionals of both $\{a_i^{\beta\,f}\}$ and $\{a_i^{\beta\,0}\}$. In particular, the average irreversible entropy production takes the form

$$\begin{aligned}\langle\mathcal{S}_{\mathrm{IRR}}\rangle=&\,\beta\sum_i\big(\lambda_i^f-\lambda_i^0\big)a_i^{\beta\,0}\\&-\beta\big\{\mathcal{F}\big[\{a_i^{\beta\,f}\}\big]-\mathcal{F}\big[\{a_i^{\beta\,0}\}\big]\big\}.\end{aligned} \tag{25}$$

We focus on sudden quenches of infinitesimal variation, where the work parameters $\{\lambda_i^0\}$ change by an elementary amount to $\{\lambda_i^0+\delta\lambda_i\}$. In this context, we can derive an explicit functional form for the average irreversible entropy production. In particular, we can expand Eq. (25) in a Taylor series and apply the HF theorem, as expressed by Eq. (8). This yields

$$\langle\mathcal{S}_{\mathrm{IRR}}\rangle=-\frac{\beta}{2}\sum_{i,j}\delta\lambda_i\delta\lambda_j\frac{\partial a_i^{\beta\,0}}{\partial\lambda_j^0}. \tag{26}$$

We emphasize that Eqs. (23) and (26) demonstrate that the mean values of work and irreversible entropy production are explicit functionals of the initial thermal densities. As discussed in the following sections, this is particularly important for extracting information about many-body systems using the KS mapping, which enables the computation of thermal electron densities within a formally noninteracting framework.

C. Fluctuation-dissipation relations in the sudden-quench limit

We now recall that classical quasiadiabatic processes follow the fluctuation-dissipation relation (FDR)

$$\langle\mathcal{S}_{\mathrm{IRR}}\rangle=\frac{\beta^2}{2}\sigma_w^2, \tag{27}$$

where $\sigma_w^2=\langle w^2\rangle-\langle w\rangle^2$ represents the variance in the PDW [16,70,71]. Recently, it has been demonstrated that for slow processes in open quantum systems, close to equilibrium, the FDR is given by Eq. (27) minus a positive, purely quantum term, which arises from the noncommutativity of the thermodynamic protocol [72,73]. Here, with the aim of obtaining an explicit functional form in terms of initial thermal densities for the second moment of the work probability distribution, we reobtain a similar generalized FDR that holds in the infinitesimal sudden-quench regime. This should not be surprising, as an adiabatic process, i.e., one that is close to equilibrium throughout, can be considered as a sequence of a large number of sudden quenches, each followed by thermalization towards the equilibrium state [73].

To this end, we focus on the second moment of the PDW. Then, we distinguish the case where the final and initial Hamiltonians share a common eigenbasis, and the case where they do not. Additional details on the following derivations are provided in Appendix C. In the specific scenario where $[\hat{\mathcal{H}}[\{\lambda_i^f\}],\hat{\mathcal{H}}[\{\lambda_i^0\}]]=0$, the second moment of the PDW is given by

$$\langle w^2\rangle_c=\sum_{i,j}\delta\lambda_i\delta\lambda_j a_i^{\beta\,0}a_j^{\beta\,0}-\frac{1}{\beta}\sum_{i,j}\delta\lambda_i\delta\lambda_j\frac{\partial a_i^{\beta\,0}}{\partial\lambda_j^0}. \tag{28}$$

Notably, Eq. (28) expresses an explicit functional of the initial mean values, independently of the amplitude of the sudden quench. Nonetheless, with an infinitesimal sudden quench, we can utilize the expressions for the average work, Eq. (23), and the average irreversible entropy production, Eq. (26), to rewrite Eq. (28) as

$$\langle w^2\rangle_c=\langle w\rangle^2+\frac{2}{\beta^2}\langle\mathcal{S}_{\mathrm{IRR}}\rangle, \tag{29}$$

This relation validates the FDR, in its classical form, as given by Eq. (27), to the leading order in $\{\delta\lambda_i\}$.

Turning to the instance where the initial and final Hamiltonians do not commute, and using Eq. (21), the second moment of the PDW is still a functional of the initial equilibrium thermal densities. Specifically, the latter can be split into the following two parts:

$$\langle w^2\rangle = \langle w^2\rangle_c + \Theta_2\big[\{a_i^{\beta\,0}\}\big], \tag{30}$$

where $\Theta_2[\{a_i^{\beta\,0}\}]$ arises directly from the incompatibility of the two Hamiltonians. A possible approximation method for this functional is provided in Sec. IV. Operating again in the infinitesimal sudden-quench limit, we can plug Eqs. (23) and (26) into Eq. (30). By doing so, we recover the generalized FDR,

$$\langle \mathcal{S}_{\rm IRR}\rangle = \frac{\beta^2}{2}\sigma_w^2 - \frac{\beta^2}{2}\Theta_2\big[\{a_i^{\beta\,0}\}\big], \tag{31}$$

which takes into account both thermal fluctuations and quantum fluctuations due to $[\hat{\mathcal{H}}[\{\lambda_i^f\}], \hat{\mathcal{H}}[\{\lambda_i^0\}]] \neq 0$.

IV. THERMAL KOHN-SHAM MAPPING FOR QUANTUM THERMODYNAMICS

The results discussed so far in previous sections are formally exact, at least in the limiting conditions of the protocols investigated for the evolution of the coupling parameters. However, as a many-body system grows in complexity, the number of interactions and possible configurations needed to determine the exact thermal density becomes computationally infeasible. To address this challenge, the KS scheme [2] provides a powerful approach within the framework of DFT for developing efficient approximations. This method relies on defining a formally noninteracting many-body system, the KS system, which is designed to replicate the same particle density as the original interacting physical system.

For systems governed by the Hamiltonian (1), and building on methods developed in earlier studies [50] at zero temperature, the KS approach can be applied as follows. We assume the existence of a set of auxiliary systems, each described by the Hamiltonian

$$\hat{\mathcal{H}}^{\rm KS} = \hat{\mathcal{H}}_0^{\rm KS} + \sum_{i=1}^{\mathcal{L}} \lambda_i^{\rm KS}\hat{A}_i, \tag{32}$$

where the one-body operator $\hat{\mathcal{H}}_0^{\rm KS}$ replaces the complex many-body term $\hat{\mathcal{H}}_0$ in Eq. (1). The KS Hamiltonian simplifies the problem by focusing on noninteracting particles in an effective potential associated to specific coupling parameters. We further assume that $\hat{\mathcal{H}}^{\rm KS}$ yields the same set of thermal densities as the original Hamiltonian:

$$\mathrm{Tr}\big\{\hat\rho_\beta^{\rm TH}[\{\lambda_i\}]\hat{A}_i\big\} = \mathrm{Tr}\big\{\hat\rho_{\beta\,\rm KS}^{\rm TH}\big[\{\lambda_i^{\rm KS}\}\big]\hat{A}_i\big\}. \tag{33}$$

In this setting, $\hat\rho_\beta^{\rm TH}$ and $\hat\rho_{\beta,\rm KS}^{\rm TH}$ denote the thermal density matrices of the original and KS systems, respectively, both parametrized by inverse temperature β and coupling parameters $\{\lambda_i\}$ and $\{\lambda_i^{\rm KS}\}$.

The MHK theorem clearly holds for the KS Hamiltonian, though with some restrictions at absolute zero temperature [49–51]. Consequently, the coupling parameters $\lambda_i^{\rm KS}$ are functionals of the thermal averages $\{a_i^\beta\}$, i.e., $\lambda_i^{\rm KS} = \lambda_i^{\rm KS}[\{a_i^\beta\}]$. At this point, the following MKS equations can be solved self-consistently for $\{a_i^\beta\}$:

$$\hat{\mathcal{H}}_0^{\rm KS} + \sum_{i=1}^{\mathcal{L}} \big(\lambda_i^{\text{H-XC}}\big[\{a_i^\beta\}\big] + \lambda_i\big)\hat{A}_i|\phi_\beta^i\rangle = \epsilon_\beta^i|\phi_\beta^i\rangle, \tag{34}$$

$$a_i^\beta = \mathrm{Tr}\big\{\hat\rho_{\beta\,\rm KS}^{\rm TH}\big[\{\lambda_i^{\text{H-XC}}\big[\{a_i^\beta\}\big] + \lambda_i\}\big]\hat{A}_i\big\}. \tag{35}$$

Here, the effective parameters $\lambda_i^{\text{H-XC}}[\{a_i^\beta\}] = \lambda_i^{\rm KS} - \lambda_i$ play the role of the Hartree (H) and exchange-correlation (XC) potentials in the usual KS mapping, which account for the effect of the many-body interaction term in $\hat{\mathcal{H}}_0$. It is worth recalling that while the eigensystem of the noninteracting KS Hamiltonian exactly reproduces the thermal density, it generally does not correspond to the eigensystem of the interacting Hamiltonian [74].

The approach outlined here is particularly useful when the one-body Hamiltonian $\hat{\mathcal{H}}_0^{\rm KS}$ has a simple form, such as in the case of a chain of interacting fermions, where $\hat{\mathcal{H}}_0^{\rm KS}$ reduces to a kinetic energy operator. In these scenarios, as is typically done within the KS framework, suitable approximations can be employed for the functionals $\lambda_i^{\text{H-XC}}[\{a_i^\beta\}]$. In other terms, any thermodynamic quantity expressed as an explicit functional of the thermal densities can be evaluated through a KS mapping, with an accuracy dictated by the approximations made for the functionals $\lambda_i^{\text{H-XC}}[\{a_i^\beta\}]$. Nonetheless, not all quantities in the MKS equations can be directly expressed as functionals of the densities. For example, the functional form of $\Theta_2[\{a_i^{\beta\,0}\}]$ in Eq. (30) requires reasonable approximations to be determined.

A. Local density approximation for $\Theta_2[\{a_i^{\beta\,0}\}]$

The local density approximation (LDA) is the simplest and most widely used approach for modeling XC effects in DFT. For instance, the LDA has been effectively employed to develop functionals for calculating the entanglement in spatially inhomogeneous many-fermion systems [75]. To construct an LDA scheme for an inhomogeneous system, it is necessary to have an analytical solution for the corresponding homogeneous problem, where all coupling parameters are equal, i.e., $\lambda_i = \lambda$. In the homogeneous case, the functional $\Theta_2[\{a_i^{\beta\,0}\}]$ reduces to $\Theta_2^{\rm HOM}[a^{\beta\,0}]$, where

$$a^{\beta\,0} = \frac{1}{\mathcal{L}}\mathrm{Tr}\left\{\hat\rho_\beta^{\rm TH}[\{\lambda_i\}]\sum_{i=1}^{\mathcal{L}}\hat{A}_i\right\}. \tag{36}$$

Based on this, the following LDA scheme can be put forward:

$$\Theta_2^{\rm LDA}\big[\{a_i^{\beta\,0}\}\big] = \sum_i \Theta_2^{\rm HOM}[a^{\beta\,0}]\big|_{a^{\beta\,0}\to a_i^{\beta\,0}}. \tag{37}$$

A crucial aspect of this implementation is that Eq. (37) approximates the fluctuations in $\Theta_2[\{a_i^{\beta,0}\}]$ arising from the incompatibility between the prequench and postquench Hamiltonians, as discussed in Sec. III C. Therefore, it is essential that the homogeneous system satisfies the condition: $[\hat{\mathcal{H}}_0, \sum_{i=1}^N \hat{A}_i] \neq 0$. Otherwise, $\Theta_2^{\rm HOM}[a^{\beta\,0}]$ would be identically zero.

B. Approximation for $\Theta_2[\{a_i^{\beta\,0}\}]$ via perturbation treatment of the KS system

The fictitious KS world is governed by a Hamiltonian that differs from the one describing the actual system under investigation. However, if the exact form of the functional $\lambda_i^{\text{H-XC}}[\{a_i^{\beta}\}]$ is known, the KS framework can accurately reproduce the density of the original interacting system. Therefore, a well-founded idea is to treat the KS Hamiltonian as a zeroth-order approximation to the "*true*" Hamiltonian [47,48,76,77]. This is because the KS Hamiltonian encapsulates key aspects of the many-body properties inherent in the real system. In this perturbationlike approach, we can express the original Hamiltonian as $\hat{\mathcal{H}} = \hat{\mathcal{H}}^{\text{KS}} + \Delta\hat{\mathcal{H}}$, where $\Delta\hat{\mathcal{H}} = \hat{\mathcal{H}} - \hat{\mathcal{H}}^{\text{KS}}$. Accordingly, any observable property $\mathcal{Q}[\{a_i^{\beta\,0}\}]$ can be expanded as

$$\mathcal{Q}\big[\big\{a_i^{\beta\,0}\big\}\big] = \mathcal{Q}^{\text{KS}}\big[\big\{a_i^{\beta\,0}\big\}\big] + \Delta\mathcal{Q}\big[\big\{a_i^{\beta\,0}\big\}\big], \tag{38}$$

where $\mathcal{Q}^{\text{KS}}[\{a_i^{\beta\,0}\}]$ represents the zeroth-order approximation of the quantity of interest. This method is particularly advantageous when the LDA scheme is not applicable. For example, if the underlying homogeneous system satisfies $[\hat{\mathcal{H}}_0, \sum_{i=1}^{N} \hat{A}_i] = 0$, the zeroth-order approximation can effectively address the incompatibility between the initial and final forms of the interacting Hamiltonian. In such cases, $\Theta_2[\{a_i^{\beta\,0}\}]$ can be approximated using the corresponding quantity calculated within the KS framework.

V. THE KOHN-SHAM SCHEME IN THE CANONICAL ENSEMBLE

In Sec. IV, we introduced a finite-temperature KS mapping, which enables the accurate evaluation of equilibrium thermal densities through iterative solutions of the self-consistent MKS equations, i.e., Eqs. (34) and (35). However, dealing with statistical systems that have a fixed number of indistinguishable particles, even within the noninteracting KS framework, presents considerable challenges [78–81], making the solution of the MKS equations computationally demanding. This complexity is one reason why finite-temperature DFT calculations typically employ the grand canonical ensemble, where the average number of particles is fixed by $\langle N\rangle = \sum_i f_\mu(\epsilon_i)$. In a many-fermion system, the Fermi-Dirac distribution $f_\mu(\epsilon_i) = (1 + e^{\beta(\epsilon_i - \mu)})^{-1}$ describes the occupation probabilities of the KS eigenstates, with ϵ_i representing the KS eigenvalues and μ the chemical potential. This framework offers the advantage of a straightforward expression for thermal electron densities: $n^{\beta}(\mathbf{r}) = \sum_i f_\mu(\epsilon_i)|\psi_i^{\text{KS}}(\mathbf{r})|^2$, based on the KS wave functions $\psi_i^{\text{KS}}(\mathbf{r})$ [82]. Here, we present a method to compute thermal densities within the canonical ensemble using the KS mapping while keeping the calculations feasible.

To elucidate our approach, we consider a system of N interacting fermions on a lattice, characterized by the Hamiltonian (1), with the specific form

$$\hat{\mathcal{H}} = \hat{\mathcal{H}}_0 + \sum_{i=1}^{\mathcal{L}} V_i \hat{n}_i. \tag{39}$$

The universal part of this Hamiltonian reads as

$$\hat{\mathcal{H}}_0 = \hat{\mathcal{T}} + \hat{\mathcal{W}}, \tag{40}$$

where

$$\hat{\mathcal{T}} = -J \sum_{i;\sigma=\uparrow,\downarrow} (\hat{c}_{i,\sigma}^{\dagger}\hat{c}_{i+1,\sigma} + \text{H.c.}) \tag{41}$$

is the kinetic term, while $\hat{\mathcal{W}}$ accounts for the two-body interaction. In Eq. (41), $\hat{c}_{i,\sigma}^{\dagger}$ and $\hat{c}_{i,\sigma}$ denote the creation and annihilation operators for a fermion with spin $\sigma = \uparrow, \downarrow$, and $\hat{n}_i = \hat{n}_{i,\uparrow} + \hat{n}_{i,\downarrow}$ is the total number operator for the ith site.

Given the form of the external potential, the thermal densities are naturally defined as $n_i^{\beta} = \text{Tr}\{\hat{\rho}_\beta^{\text{TH}}[\{V_i\}]\hat{n}_i\}$. According to the MHK theorem, the following correspondence holds:

$$\{V_i\} \iff \big\{n_i^{\beta}\big\} \iff \hat{\rho}_\beta^{\text{TH}} \equiv \hat{\rho}_\beta^{\text{TH}}\big[\big\{n_i^{\beta}\big\}\big]. \tag{42}$$

As remarked in Sec. IV, there exists a KS system having exactly the same set of thermal densities as the original interacting system. The corresponding KS Hamiltonian is

$$\hat{\mathcal{H}}^{\text{KS}} = \hat{\mathcal{T}} + \sum_{i=1}^{\mathcal{L}} \big(V_i^{\text{H-XC}}\big[\big\{n_i^{\beta}\big\}\big] + V_i\big)\hat{n}_i. \tag{43}$$

At this point, we seek a more computationally tractable equation for the thermal densities than Eq. (35). In particular, we build on previous research [78,79] that examined the canonical partition function for N noninteracting fermions. These studies enable us to express the canonical partition function for the KS fermions using the following recursive formula:

$$\mathcal{Z}_N = \frac{1}{N}\sum_{m=0}^{N}(-1)^{m-1}\mathcal{Z}_1(m\beta)\mathcal{Z}_{N-m}(\beta), \tag{44}$$

where $\mathcal{Z}_1(0) = 1$ and $\mathcal{Z}_1(m\beta) = \sum_i e^{-m\beta\epsilon_i}$ for $m > 1$.

Given the structure of the KS Hamiltonian (43), the partition function for a KS system with $N_\uparrow$ spin-up and $N_\downarrow$ spin-down fermions becomes $\mathcal{Z}_N^{\text{KS}} = \mathcal{Z}_{N_\uparrow}^{\text{KS}}\mathcal{Z}_{N_\downarrow}^{\text{KS}}$, with particle-number conservation ensured by $N = N_\uparrow + N_\downarrow$. The corresponding equilibrium free energy is then $\mathcal{F}^{\text{KS}} = -\frac{1}{\beta}\log(\mathcal{Z}_N^{\text{KS}})$, from which the equilibrium thermal densities can be extracted using the HF theorem as

$$n_i^{\beta} = \frac{\partial\mathcal{F}^{\text{KS}}}{\partial V_i^{\text{KS}}}. \tag{45}$$

The combination of Eqs. (45) and (34) forms the self-consistent foundation of our finite-temperature KS approach, which, in principle, exactly reproduces the thermal densities of the original interacting system.

VI. A NOTABLE EXAMPLE

This section is dedicated to validating our finite-temperature KS approach, as defined by Eqs. (34) and (45), within the context of the Hubbard model [83–85]. Specifically, we examine a scenario where electrons are influenced by an inhomogeneous external potential dependent on the parameter v_0. The system Hamiltonian is expressed as

$$\hat{\mathcal{H}} = \hat{\mathcal{H}}_0 + \sum_{i=1}^{\mathcal{L}} V_i(\text{v}_0)\hat{n}_i, \tag{46}$$

where $V_i(\mathrm{v}_0) = f_i \mathrm{v}_0$ with the dimensionless set $\{f_i\}$ that defines the spatial shape of the external potential along the chain. Here $\hat{\mathcal{H}}_0$ takes the form given in Eq. (40), with the two-body interaction term given by

$$\hat{\mathcal{W}} = \sum_{i=1}^{\mathcal{L}} U \hat{n}_{i,\uparrow} \hat{n}_{i,\downarrow}. \tag{47}$$

As described in Sec. III the system is initially prepared in the Gibbs state $\hat{\rho}_\beta^{\mathrm{TH}}[\{n_i^\beta\}]$. Subsequently, it is decoupled from the thermal bath and undergoes an instantaneous quench in the work parameter, with amplitudes $\delta V_i = f_i \delta \mathrm{v}_0$.

We focus on the half-filled Hubbard model, with the total spin along the z direction set to zero. Our analysis considers two external potentials. One that decreases linearly along the chain,

$$\hat{\mathcal{V}}_{\mathrm{EXT}} = \sum_{i=1}^{\mathcal{L}} \left[\mathrm{v}_0 - \frac{2\mathrm{v}_0(i-1)}{\mathcal{L}-1} \right] \hat{n}_i, \tag{48}$$

and another one with a harmonic dependence,

$$\hat{\mathcal{V}}_{\mathrm{EXT}} = \sum_{i=1}^{\mathcal{L}} \frac{1}{2} \mathrm{v}_0 \left[i - \frac{\mathcal{L}+1}{2} \right]^2 \hat{n}_i. \tag{49}$$

We begin by analyzing the exact results for the Hubbard dimer, as presented in Sec. VI A. We then compare these results with those obtained from our KS mapping, as detailed in Sec. VI B and further explored in Sec. VI C. Next, we extend our study to longer Hubbard chains probed by the linear potential defined in Eq. (48), as outlined in Secs. VI B and VI D. In particular, in Sec. VI B, we compare exact results for systems with up to eight sites with corresponding ones from our KS mapping. Finally, in Secs. VI D 1 and VI D 2, we investigate the impact of electron-electron interactions on work extraction in longer chains, considering both linear and harmonic potentials given in Eqs. (48) and (49).

A. Exact results for the Hubbard dimer

In the two-particle subspace with total spin zero along the z axis, the Hamiltonian (46) characterizes a two-site Hubbard chain and is represented by the matrix

$$\hat{\mathcal{H}} \doteq \begin{pmatrix} U + 2V_1 & -J & J & 0 \\ -J & V_1 + V_2 & 0 & -J \\ J & 0 & V_1 + V_2 & J \\ 0 & -J & J & U + 2V_2 \end{pmatrix}, \tag{50}$$

in the basis $\{|\uparrow\downarrow, 0\rangle, |\uparrow, \downarrow\rangle, |\downarrow, \uparrow\rangle, |0, \uparrow\downarrow\rangle\}$. This straightforward, exactly solvable model exhibits a diverse range of physical phenomena [48,86–88], including a precursor to the Mott metal-insulator transition and, influenced by the external potential, a precursor to the ionic insulator transition. The two transitions are in competition, with the former favoring single-site occupation and the latter promoting double-site occupation. The metal phase emerges in the narrow region where $U \sim 2\mathrm{v}_0$, driven by the interplay of the interaction term and the external potential.

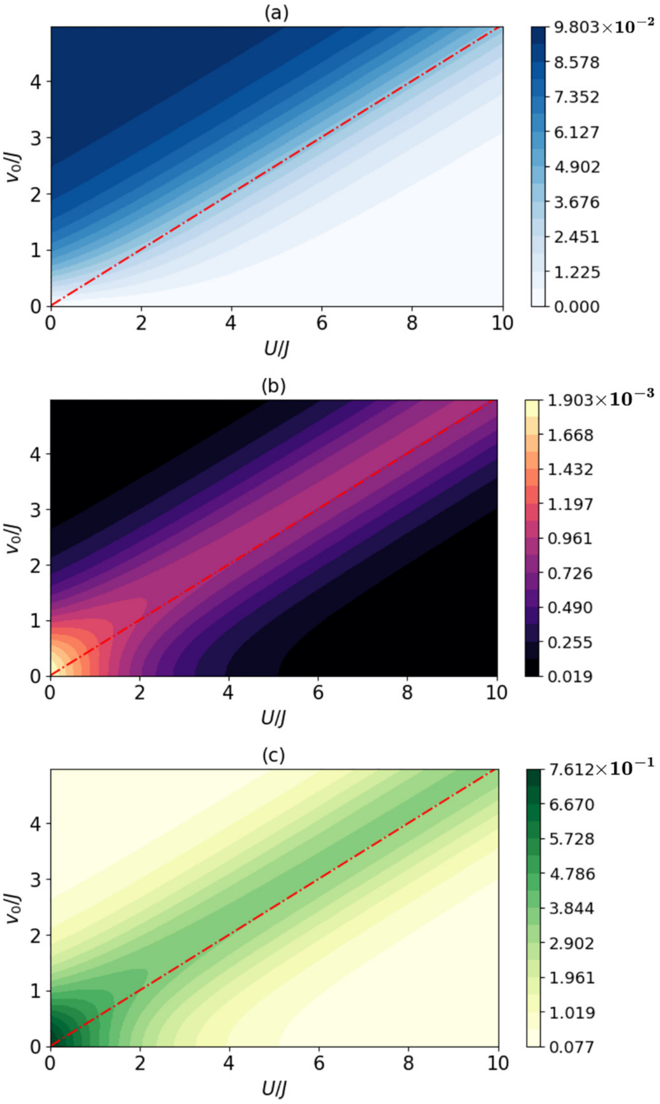

FIG. 1. (a) Average extracted quantum work $\langle w \rangle_{\mathrm{EX}}$, (b) average irreversible entropy production $\langle \mathcal{S}_{\mathrm{IRR}} \rangle$, and (c) the first derivative of the thermal density n_i^β with respect to the work parameter v_0, for a Hubbard dimer at the inverse temperature $\beta = 1/J$ and a sudden quench of amplitude $\delta \mathrm{v}_0 = 0.05J$. In all panels, the red dashed-dotted line represents the condition $U = 2\mathrm{v}_0$.

In Fig. 1(a), we examine the average extracted work $\langle w \rangle_{\mathrm{EX}} = -\langle w \rangle$ as a function of U and v_0, following a sudden quench of amplitude $\delta v = 0.05J$. For $U > 2\mathrm{v}_0$, the system enters the Mott insulating phase, leading to a decrease in the extractable work as the interaction strength U increases. In this phase, double occupancy of sites becomes energetically unfavorable, rendering work extraction through the external potential quench impractical. This behavior can be understood by examining the thermal densities in the limit of large U: for $U \gg 2\mathrm{v}_0$, we have $n_1^\beta \sim n_2^\beta \sim 1$, which, according to Eq. (23), results in $\langle w \rangle \sim 0$. Conversely, for $U < 2\mathrm{v}_0$, the system is in the ionic insulating phase, where the extractable work increases as U decreases, reaching its maximum value as U approaches zero. This is because for $U \ll 2\mathrm{v}_0$ we find $n_1^\beta \sim 2$ and $n_2^\beta \sim 0$, leading to $\langle w \rangle \sim -2\delta \mathrm{v}_0$ as per Eq. (23).

In Fig. 1(b), we show the average irreversible entropy production $\langle \mathcal{S}_{\mathrm{IRR}} \rangle$ for the same process. As expected, $\langle \mathcal{S}_{\mathrm{IRR}} \rangle$ exhibits a pronounced peak in the metallic region separating

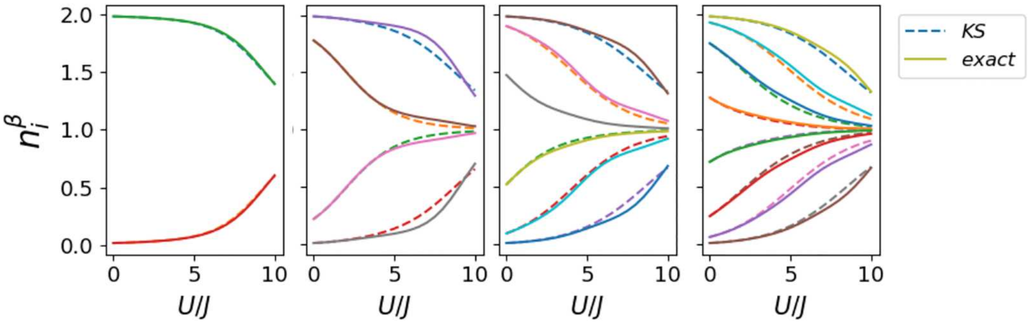

FIG. 2. Thermal densities obtained through exact diagonalization of the Hubbard Hamiltonian (46) compared with those from our KS mapping, as a function of U for $\mathrm{v}_0 = 5J$ and $\beta J = 1$. The percentage error for chains of two, four, six, and eight sites is 0.7%, 3.7%, 2.28%, and 1.78%, respectively.

the Mott insulating phase from the ionic insulating phase. This behavior can be understood through the dependence of the average irreversible entropy production on the thermal densities, as described in Eq. (26). The thermal densities are sensitive to small variations in the work parameter v_0 when $U \sim 2\mathrm{v}_0$, which is also reflected in the peak observed in the derivatives of the thermal density with respect to v_0, shown in Fig. 1(c).

B. Thermal KS mapping for Hubbard chains

To evaluate the thermodynamic quantities of interest for the Hubbard model using our thermal KS scheme, the first step is to construct an accurate approximation for the H-XC potential. Some previous studies [8,88–90] provide a robust framework for this construction. Furthermore, in the context of the Anderson model for a single nonmagnetic impurity coupled to two leads, it has been demonstrated that the impurity Hamiltonian, modeled as a single-site Hubbard model, is v representable in the noninteracting case. This allows for the derivation of an analytical form for the XC potential [91].

To proceed further, we treat the Hubbard chain as a collection of single sites coupled by the kinetic term (41). Following the LDA, we approximate the KS potential as

$$\begin{aligned} V_i^{\text{KS}}[\{n_i^\beta\}] &\simeq V_i + V_{\text{SS}}^{\text{H-XC}}[n_i^\beta] \\ &= V_i + U + \frac{1}{\beta}\ln \Gamma_U^\beta[n_i^\beta], \end{aligned} \tag{51}$$

where $V_{\text{SS}}^{\text{H-XC}}[n^\beta]$ is the single-site H-XC potential, derived from the nonmagnetic impurity Anderson model [91]. Further details of this construction are provided in Appendix D, with the explicit form of Γ_U^β given in Eq. (D11). It is worth mentioning that Eq. (51) can be viewed as a simplified version of the LDA scheme implemented in [90], which utilized the solution of the homogeneous problem via the thermal Bethe ansatz.

With a reliable approximation for the H-XC potential in hand, we can solve our thermal KS equations

$$\left\{\hat{\mathcal{T}} + \sum_i V^{\text{KS}}[n_i^\beta]\hat{n}_i\right\}|\phi_\beta^i\rangle = \epsilon_\beta^i|\phi_\beta^i\rangle, \tag{52}$$

$$n_i^\beta = -\frac{2}{\beta}\frac{\partial \log\left(\mathcal{Z}_{N_\uparrow}^{\text{KS}}\right)}{\partial V_i^{\text{KS}}}, \tag{53}$$

adapted from Eqs. (35) and (45), to obtain the set of thermal densities.

Figure 2 illustrates a comparison between the thermal densities obtained through exact diagonalization of Eq. (46) and those obtained using our KS mapping, as a function of the interaction parameter U. This analysis covers chains with up to eight sites, using the external potential defined in Eq. (48), with $\mathrm{v}_0 = 5J$ and the inverse temperature $\beta = 1/J$. To assess the accuracy of the approximation, we use the density metric discussed in [92]

$$\mathcal{D}(\{n_i^\beta\}, \{n_i^{\beta\text{KS}}\}) = \frac{1}{2N}\sum_i |n_i^\beta - n_i^{\beta\,\text{KS}}|, \tag{54}$$

where the scaling factor $2N$ represents the maximum possible distance between the two sets of thermal densities, ensuring that the distances lie within the range [0,1]. For the chosen density metric and parameters, the percentage error for all the chain lengths is less than 3.7%.

Now that the validity of the approximation for the thermal densities is established, we can proceed to evaluate the thermodynamic quantities of interest for which an explicit functional is available.

C. Thermal KS mapping for the Hubbard dimer

Here we leverage our KS mapping, defined by the above derived self-consistent equations (52) and (53), to compute various statistical moments for the Hubbard dimer and compare these with the exact solution discussed in Sec. VI A. Specifically, we focus on evaluating the first and second moments of the PDW and the first moment of the PDEP.

We determine the average extractable work $\langle w\rangle_{\text{EX}} = -\langle w\rangle$, using Eq. (23), and the average irreversible entropy production $\langle \mathcal{S}_{\text{IRR}}\rangle$, using Eq. (26), from the thermal densities obtained by solving Eqs. (52) and (53). Figures 3(a) and 3(b) display $\langle w\rangle_{\text{EX}}$ and $\langle \mathcal{S}_{\text{IRR}}\rangle$, respectively, as functions of the interaction strength U and the work parameter v_0. The system is set at an inverse temperature of $\beta = 1/J$ with a sudden quench of amplitude $\delta\mathrm{v}_0 = 0.05J$. The computed results are in excellent agreement with the exact results shown in Figs. 1(a) and 1(b), validating the reliability and accuracy of our KS framework for the Hubbard dimer. This approach becomes comparatively less precise when computing the second moment of the PDW. As outlined in Sec. III, $\langle w^2\rangle$ consists of two contributions:

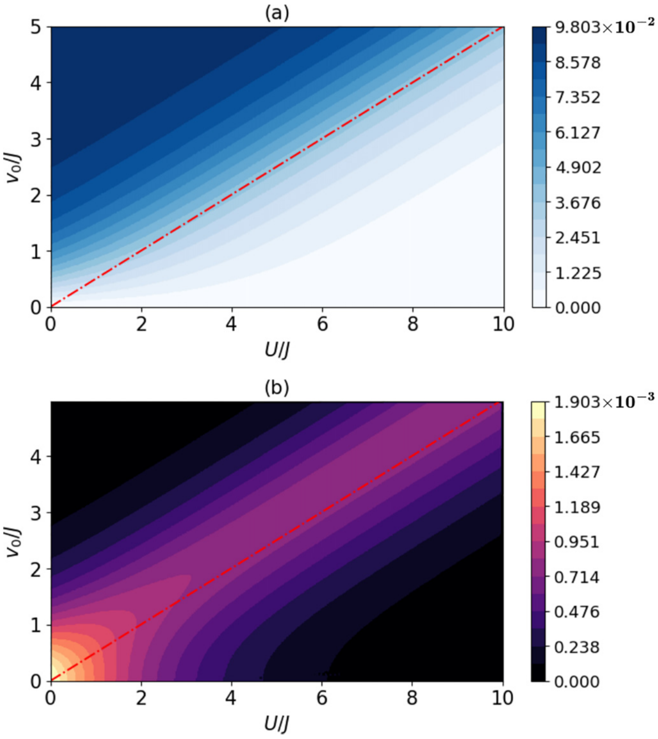

FIG. 3. Mean values of (a) the extracted quantum work $\langle w\rangle_{\text{EX}}$ and (b) the irreversible entropy production $\langle \mathcal{S}_{\text{IRR}}\rangle$, for a Hubbard dimer at $\beta = 1/J$ and $\delta\text{v}_0 = 0.05J$. In both panels, the red dashed line corresponds to $U = 2\text{v}_0$.

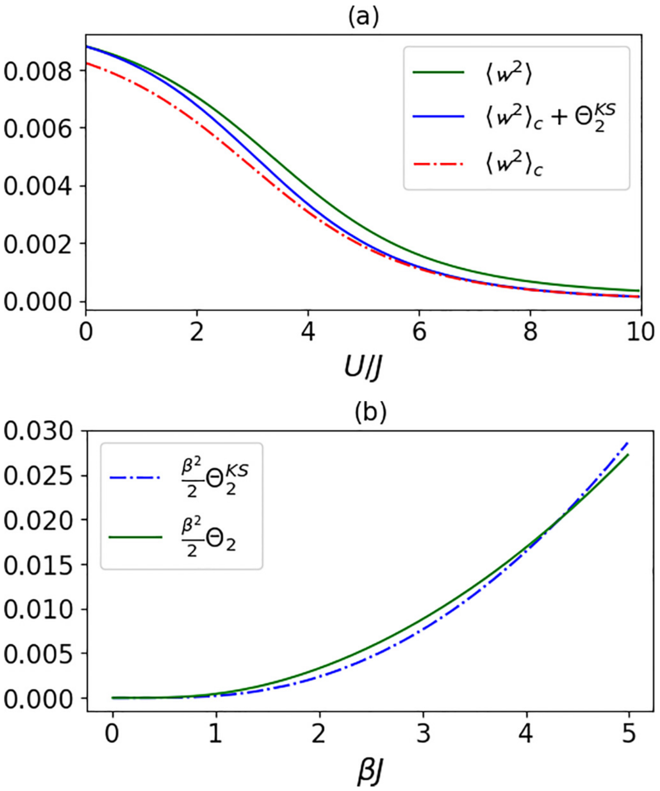

FIG. 4. (a) Second moment of the PDW for the Hubbard dimer $\langle w^2\rangle$ as a function of the interaction strength U, at the inverse temperature of $\beta = 1/J$. This exact result is compared with the KS result $\langle w^2\rangle_c + \Theta_2^{\text{KS}}$ and the contribution $\langle w^2\rangle_c$ alone. (b) Noncommutative functional Θ_2 evaluated exactly and via our KS scheme as a function of the inverse temperature β, for $U = 3J$. In both panels, the sudden-quench protocol $\text{v}_0 = 2.00J \to \text{v}_f = 2.05J$ is considered, corresponding to a sudden quench of amplitude $\delta\text{v}_0 = 0.05J$.

$\langle w^2\rangle_c$, which is an explicit functional of the thermal density, as defined in Eq. (28), and Θ_2, introduced in Eqs. (30) and (31), which addresses the incompatibility of the prequench and postquench Hamiltonians. Currently, there is no available explicit functional form for Θ_2. Besides, the Hubbard model falls into the category where an LDA approach for this contribution cannot be implemented because $[\hat{\mathcal{H}}_0, \sum_{i=1}^{N}\hat{n}_i] = 0$. Thus, we use the zeroth-order approximation described in Sec. V B, and apply the generalized FDR of Eq. (31) to estimate the noncommutative functional as $\Theta_2[\{n_i^{\beta,0}\}] \approx \Theta_2^{\text{KS}}[\{n_i^{\beta,0}\}]$. Figure 4(a) shows $\langle w^2\rangle$, as calculated within the analytic framework of the Hubbard dimer (green line). This exact result is compared with $\langle w^2\rangle_{\text{KS}} = \langle w^2\rangle_c + \Theta_2^{\text{KS}}$, obtained via our KS mapping (blue line), and with $\langle w^2\rangle_c$ alone (red line). In particular, $\langle w^2\rangle$, $\langle w^2\rangle_{\text{KS}}$, and $\langle w^2\rangle_c$ are plotted as a function of U at an intermediate temperature of $\beta J = 1$ and a sudden quench of amplitude $\delta\text{v}_0 = 0.05J$. We observe that our KS approach becomes less accurate as the value of U increases above $\sim 2J$. In fact, for $U \gtrsim 5$ $\langle w^2\rangle_{\text{KS}}$ appears indistinguishable from $\langle w^2\rangle_c$, and the contribution from the incompatibility between the prequench and postquench KS Hamiltonians vanishes. The underlying reason is that, as the parameter U increases, the thermal densities n_1^{β} and n_2^{β} tend to be equal, making $V^{\text{KS}}[n_i^{\beta}] \approx V_{\text{SS}}^{\text{H-XC}}[n_i^{\beta}]$, and thus $[\hat{\mathcal{H}}, \sum_i V^{\text{KS}}[n_i^{\beta}]\hat{n}_i] = 0$. One potential refinement of our approximation, while remaining within the framework of the KS zero-order approximation, could be to construct an H-XC potential inspired by the generalized gradient approximation (GGA) [93–95]. Alternatively, another strategy involves maintaining the selected H-XC potential while enhancing the approximation by extending beyond the KS zero-order framework, specifically within the context of many-body perturbation theory, where the unperturbed Hamiltonian is the KS Hamiltonian. These refinements would improve results also for large U values, where the local densities tend to become homogeneous, which would induce the prequench and postquench Hamiltonian to commute. In particular, the GGA functional should improve the detection of slight local variation of the density in the large U limit.

To assess the accuracy of our KS scheme as a function of temperature, Fig. 4(b) displays $\Theta_2^{\text{KS}}[\{n_i^{\beta,0}\}]$ and $\Theta_2[\{n_i^{\beta,0}\}]$ as functions of βJ for $U = 3J$. The two results exhibit values that are close to each other and show similar trends, indicating that the approximation remains reliable across the explored temperature range for the specified value of U.

D. Average extracted work for Hubbard chains with varying length

We finally focus on the possibility of extracting work from an interacting many-body system. According to Eq. (23) the

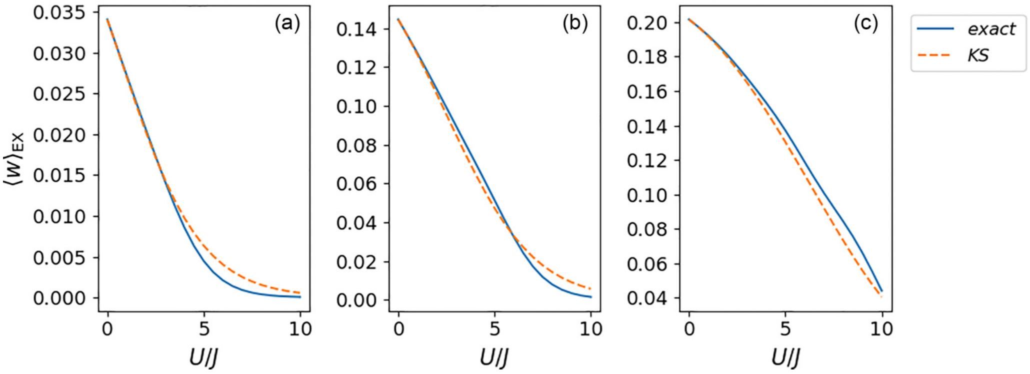

FIG. 5. Average work extracted with the linear potential defined in Eq. (48) for a sudden quench of amplitude $\delta \mathrm{v}_0 = 0.05J$. Exact results obtained via diagonalization of the Hamiltonian (46) are compared with those from our KS mapping for a chain with eight sites. The comparisons are made for three different values of v_0, namely, (a) $\mathrm{v}_0 = 0.5J$, (b) $\mathrm{v}_0 = 2.5J$, and (c) $\mathrm{v}_0 = 5J$. The corresponding maximum errors are (a) $0.0019J$, (b) $0.0063J$, and (c) $0.0113J$.

average work for the Hubbard chain is given by

$$\langle w \rangle = \sum_i f_i \delta \mathrm{v}_0 n_i^\beta, \tag{55}$$

where the sign of the quenching amplitude $\delta \mathrm{v}_0$ and the behavior of the thermal densities n_i^β determine whether the work can be extracted, meaning $\langle w \rangle < 0$. In this context, the thermal densities are strongly influenced by the interplay between the external potential, characterized by the set of parameters $\{f_i \mathrm{v}_0\}$, and the many-body interaction. As observed for the Hubbard dimer in Sec. VI A, the system can experience different phases depending on the relative magnitudes of U and v_0. For $\mathrm{v}_0 \gg U$, a band insulator phase emerges, where double occupancy is favored. For $U \gg \mathrm{v}_0$, a Mott insulator phase occurs, where the strong interaction inhibits double occupancy. When U and v_0 are comparable, a metallic phase manifests, due to the competition between the external potential and the many-body interaction. In this respect, the external potential plays a crucial role in determining which phase occurs in different regions of the chain. We here demonstrate that the external potential can actually enhance the effects of many-body interactions, thereby facilitating the extraction of work, either by driving the system towards the band insulator phase or by shifting it towards the Mott insulator phase. As outlined earlier in this section, we focus our analysis on the linear decreasing potential (48) and the harmonic potential (49), establishing that the ability to extract work from many-body interactions is highly dependent on the nature of the external potential.

1. Linear potential

We begin by considering the external potential that decreases linearly along the chain. In Fig. 5, we compare the extracted work, calculated exactly and using our KS mapping for an eight-site chain. As expected, given the good approximation for the thermal densities, discussed in Fig. 2, the two results show excellent agreement. Figure 5 also illustrates that for a fixed value of v_0, and a quench of amplitude $\delta \mathrm{v}_0 > 0$, the extractable work decreases monotonically as the interaction strength U increases.

This behavior is further explored in the context of a 16-site chain. In Fig. 6, the extracted work is shown as a function of U and v_0. With the system prepared in the band insulator phase, near-double occupancy is favored at the sites in the second half of the chain, although this is partially masked by finite-temperature effects. Performing a quench of the work parameter with an amplitude $\delta \mathrm{v}_0 > 0$ further promotes this double occupancy, which translates into the opportunity of extracting the maximum possible work:

$$\langle w \rangle \sim 2\delta \mathrm{v}_0 \sum_{i=\mathcal{L}/2}^{\mathcal{L}} \left[1 - \frac{2(i-1)}{\mathcal{L}-1}\right] = -\frac{(\mathcal{L}^2-4)\delta \mathrm{v}_0}{2(\mathcal{L}-1)}. \tag{56}$$

Conversely, at a fixed initial v_0, as the interaction parameter increases, less and less work can be extracted from the system. This occurs because the electron-electron interaction opposes double occupancy, counteracting the effect of the quench $\mathrm{v}_0 \to \mathrm{v}_0 + \delta \mathrm{v}_0$ that would otherwise favor it. In the strongly interacting limit, where each $n_i^\beta \sim 1$, the external potential form prevents work from being extracted at all:

$$\langle w \rangle \sim \delta \mathrm{v}_0 \sum_{i=1}^{\mathcal{L}} \left[1 - \frac{2(i-1)}{\mathcal{L}-1}\right] = 0. \tag{57}$$

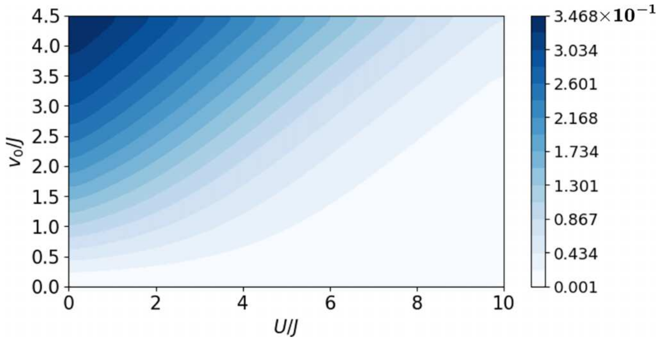

FIG. 6. Average work extracted from a Hubbard chain with 16 sites, probed by the linear potential of Eq. (48). The system is at an inverse temperature of $\beta = 1/J$, with a sudden quench of amplitude $\delta \mathrm{v}_0 = 0.05J$.

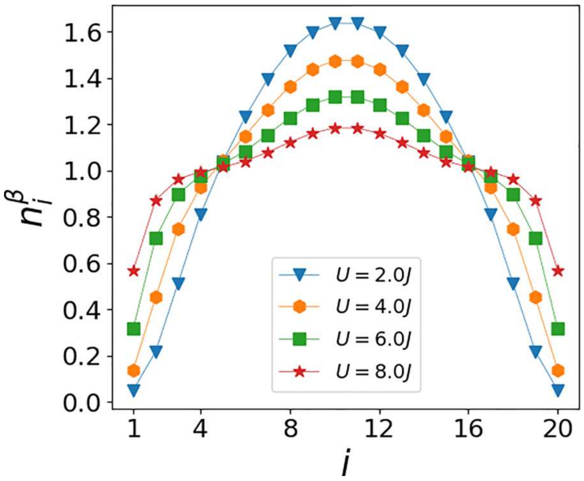

FIG. 7. Spatial distribution of the thermal densities for a fixed $\mathrm{v}_0 = 0.175J$ and four different values of U at an inverse temperature $\beta J = 1$.

In summary, for a positive quench of amplitude $\delta\mathrm{v}_0 > 0$, the work lies in the range $-\frac{(\mathcal{L}^2-4)\delta\mathrm{v}_0}{2(\mathcal{L}-1)} \leqslant \langle w\rangle \leqslant 0$. This indicates that work can be extracted starting from any initial state, with many-body interactions generally impeding this extraction. On the other hand, for quenches of negative amplitudes, $\delta\mathrm{v}_0 < 0$, the work is positive covering the range $0 \leqslant \langle w\rangle \leqslant \frac{(\mathcal{L}^2-4)|\delta\mathrm{v}_0|}{2(\mathcal{L}-1)}$.

2. Harmonic potential

We now turn our attention to the scenario where electrons are subjected to a parabolic (harmonic) potential. The impact of this potential on the thermal densities $\{n_i^\beta\}$ is illustrated in Fig. 7 for a fixed v_0 and four distinct values of U on a 20-site chain. It is evident that the primary impact of many-body interactions is to suppress the double occupancy at the center of the chain favored by the external potential.

Unlike the linear potential case, the parabolic potential does not allow work extraction via a quench that drives the system toward a band insulator phase, regardless of the values of v_0 and U, i.e., independent of the phase in which the system resides before the quench. In other words, no extraction of work is possible for a quench in which the parabola amplitude is changed from v_0 to $\mathrm{v}_0 + \delta\mathrm{v}_0$. Conversely, if the quench increases the parabola amplitude, the average work $\langle w\rangle$ is negative for any initial values of v_0 and U, see Fig. 8 meaning that work can always be extracted. The underlying reason is that the Coulomb repulsion and the widening of the parabola do not compete but rather favor the condition $\{n_i^\beta \sim 1\}$. In contrast to the linear potential, stronger many-body interactions here result in more work being extracted. Specifically, in the deep Mott phase, the extractable work reaches its maximum possible value.

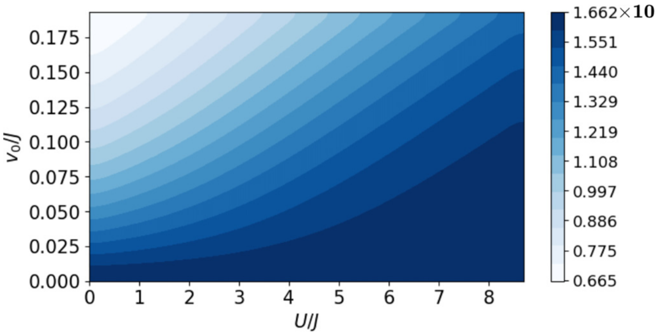

FIG. 8. Mean value of the quantum work extracted from a Hubbard chain subjected to a harmonic potential, at an inverse temperature $\beta = 1/J$, following a quench with amplitude $\delta\mathrm{v}_0 = 0.05J$.

VII. CONCLUSIONS

In this work, we have explored the thermodynamics of many-body systems through the lens of the MHK theorem and a finite-temperature KS mapping. In particular, utilizing the MHK theorem, we demonstrated that the PDW and the PDEP, along with their characteristic functions, can be expressed as functionals of the thermal densities. This insight turned to be particularly powerful as it provides a unified framework for analyzing the statistics of work and irreversible entropy production in the context of sudden quenches of small amplitudes. Specifically, we derived simple analytical expressions for the first moments of the PDW and the PDEP that are functionals of the thermal densities and their derivatives. For the second moment of the PDW, we identified and separated two distinct contributions: $\langle w^2\rangle_c$, a classical-like term, and $\Theta_2[n_i^{\beta,0}]$, a purely quantum contribution arising from the noncommutativity of the prequench and postquench Hamiltonians. This separation enabled us to establish a generalized FDR in the sudden-quench regime to the lowest order in the amplitude parameters $\delta\lambda_i$. We then introduced a KS mapping as a promising approach for studying the thermodynamics of many-body systems, especially when explicit functionals for thermodynamic quantities are unavailable. In Sec. V, we developed a method to evaluate thermal densities using the KS scheme within the canonical ensemble framework, thereby bypassing the need to construct the many-body Gibbs state explicitly. The proposed method was validated on out-of-equilibrium thermodynamics of the Hubbard model under the influence of a nonhomogeneous external potential. We assessed the accuracy of the KS mapping by comparing the exact thermal densities with those obtained via the KS approach for chains of up to eight sites. Furthermore, we explored the quantum thermodynamics of the quenched Hubbard dimer, illustrating the applicability and limitations of the KS mapping when an explicit functional is unavailable. Our investigation into the role of many-body interactions in work extraction revealed that the KS mapping, combined with our general findings, provides a robust framework for analyzing the thermodynamic properties of complex quantum systems. The principles of zero-temperature density-functional theory have been demonstrated for a set of model Hamiltonians, including the Heisenberg model and the XXZ model (see, e.g., [74]). In this respect, the set of our results independent from the model could be directly applied also to these other Hamiltonians. In summary, our KS mapping, along with the insights gained from the MHK theorem, offers a powerful tool for studying the thermodynamics of many-body systems in out-of-equilibrium scenarios. As quantum technologies continue to advance, our results could play a significant role in the development of efficient quantum thermal devices, providing a pathway to explore thermodynamic properties in regimes where traditional methods fall short.

ACKNOWLEDGMENTS

This research was partially supported by Centro Nazionale di Ricerca in High-Performance Computing, Big Data and Quantum Computing, PNRR 4 2 1.4, CI CN00000013, CUP H23C22000360005, and by the PNRR MUR Project No. PE0000023-NQSTI. A.P. would like to thank the Erasmus+ programme and the kind hospitality of the University of York.

APPENDIX A: UNIQUE MAPPING FOR CLOSED QUANTUM SYSTEMS

We present here the MHK theorem for closed quantum systems described by Hamiltonians of the form (1). Let us consider the following Hamiltonians:

$$\hat{\mathcal{H}} = \hat{\mathcal{H}}_0 + \sum_{i=1}^{\mathcal{L}} \lambda_i \hat{A}_i = \hat{\mathcal{H}}[\{\lambda_i\}] \tag{A1}$$

and

$$\hat{\mathcal{H}}' = \hat{\mathcal{H}}_0 + \sum_{i=1}^{\mathcal{L}} \lambda'_i \hat{A}_i = \hat{\mathcal{H}}[\{\lambda'_i\}], \tag{A2}$$

respectively, associated to the sets of external parameters $\{\lambda_i\}$ and $\{\lambda'_i\}$ of fixed length $\mathcal{L}$, which differ by more than a site-independent constant. The free energy corresponding to $\hat{\mathcal{H}}$, as given by Eq. (4), is minimized by the Gibbs state $\hat{\rho}_\beta^{\text{TH}} = \hat{\rho}_\beta^{\text{TH}}[\{\lambda_i\}]$. We assume that this state is unique. Similarly, the free energy corresponding to $\hat{\mathcal{H}}$ is minimized by $\hat{\rho}_\beta^{\text{TH}'} = \hat{\rho}_{\beta'}^{\text{TH}}[\{\lambda'_i\}]$. We also assume that this state is unique. Given the nontrivial choice for the two sets of external parameters, the two above introduced thermal states must be different: $\hat{\rho}_\beta^{\text{TH}'} \neq \hat{\rho}_\beta^{\text{TH}}$. Suppose that both $\{\lambda_i\}$ and $\{\lambda'_i\}$ result in the same set of mean values $\{a_i^\beta\}$. The two Hamiltonians are simply related by

$$\hat{\mathcal{H}}' = \hat{\mathcal{H}} + \sum_{i=1}^{\mathcal{L}} (\lambda'_i - \lambda_i)\hat{A}_i. \tag{A3}$$

Consequently, the equilibrium free energy corresponding to the Hamiltonian (A2) can be expressed as

$$\begin{aligned}\mathcal{F}'\big[\hat{\rho}_\beta^{\text{TH}'}\big] &= \text{Tr}\left\{\hat{\rho}_\beta^{\text{TH}'}\left[\hat{\mathcal{H}} + \sum_{i=1}^{\mathcal{L}}(\lambda'_i - \lambda_i)\hat{A}_i + \frac{\ln \hat{\rho}_\beta^{\text{TH}'}}{\beta}\right]\right\}\\ &= \mathcal{F}\big[\hat{\rho}_\beta^{\text{TH}'}\big] + \sum_{i=1}^{\mathcal{L}}(\lambda'_i - \lambda_i)a_i^\beta. \end{aligned}\tag{A4}$$

By the minimization principle of the equilibrium free energy, we must have $\mathcal{F}[\hat{\rho}_\beta^{\text{TH}'}] > \mathcal{F}[\hat{\rho}_\beta^{\text{TH}}]$, which leads to the inequality

$$\mathcal{F}'\big[\hat{\rho}_\beta^{\text{TH}'}\big] > \mathcal{F}\big[\hat{\rho}_\beta^{\text{TH}}\big] + \sum_{i=1}^{\mathcal{L}}(\lambda'_i - \lambda_i)a_i^\beta. \tag{A5}$$

This inequality remains valid when primed and unprimed quantities are interchanged, yielding

$$\mathcal{F}\big[\hat{\rho}_\beta^{\text{TH}}\big] > \mathcal{F}'\big[\hat{\rho}_\beta^{\text{TH}'}\big] + \sum_{i=1}^{\mathcal{L}}(\lambda_i - \lambda'_i)a_i^\beta. \tag{A6}$$

As in the original formulation of the first HK theorem [1], Eqs. (A5) and (A6) lead to the absurd conclusion that $\mathcal{F}'[\hat{\rho}_\beta^{\text{TH}'}] + \mathcal{F}[\hat{\rho}_\beta^{\text{TH}}] > \mathcal{F}[\hat{\rho}_\beta^{\text{TH}}] + \mathcal{F}'[\hat{\rho}_\beta^{\text{TH}'}]$. Therefore, one and only one set of nontrivial external parameters, $\{\lambda_i\}$, can result in a given set of mean values, $\{a_i^\beta\}$, provided that the equilibrium Gibbs state is unique. As a corollary, since $\{a_i^\beta\}$ uniquely determines $\{\lambda_i\}$, which in turn determines $\hat{\rho}_\beta^{\text{TH}}$, the thermal state is also a functional of the set $\{a_i^\beta\}$. Specifically,

$$\{\lambda_i\} \iff \big\{a_i^\beta\big\} \iff \hat{\rho}_\beta^{\text{TH}} \equiv \hat{\rho}_\beta^{\text{TH}}\big[\big\{a_i^\beta\big\}\big]. \tag{A7}$$

As a final note, we observe that this proof is based on the variational principle satisfied by the equilibrium free energy. Similarly, one could use an approach based on the constrained-search technique [96], thus removing the hypothesis on the uniqueness of the Gibbs thermal state, as it has been done in a previous study conducted at zero temperature [50].

APPENDIX B: AVERAGE WORK AND IRREVERSIBLE ENTROPY PRODUCTIONS FOR GENERAL FINITE-TIME PROTOCOLS

The Runge-Gross theorem for statistical mixtures [97] ensures that the temporal evolution of an initial thermal state $\hat{\rho}_\beta^{\text{TH}}$ is a functional of the out-of-equilibrium electron density $n_\tau(\mathbf{r})$, i.e.,

$$\begin{aligned}\hat{\rho}(\tau) &= \hat{\mathcal{U}}(\tau,0)\hat{\rho}_\beta^{\text{TH}}\big[n_0^\beta(\mathbf{r})\big]\mathcal{U}^\dagger(\tau,0)\\ &= \hat{\rho}_\tau\big[n_\tau(\mathbf{r}), n_0^\beta(\mathbf{r})\big].\end{aligned}\tag{B1}$$

Previous studies [98,99] have shown that for pure states, an analogous form of the Runge-Gross theorem holds for systems driven by the Hamiltonians (1). Assuming that the same proof can be extended to statistical mixtures, Eq. (B1) becomes

$$\begin{aligned}\hat{\rho}(\tau) =& \hat{\mathcal{U}}(\tau,0)\hat{\rho}_\beta^{\text{TH}}\big[\big\{a_i^{\beta\,0}\big\}\big]\mathcal{U}^\dagger(\tau,0)\\ &= \hat{\rho}_\tau\big[\big\{a_i^{\beta\,\tau}\big\}, \big\{a_i^{\beta\,0}\big\}\big].\end{aligned}\tag{B2}$$

By defining the out-of-equilibrium free energy as in Eq. (4), the average work and the irreversible entropy production, respectively, become

$$\langle w \rangle = \mathcal{F}[\hat{\rho}(\tau)] - \mathcal{F}\big[\hat{\rho}_\beta^{\text{TH}\,0}\big], \tag{B3}$$

with $\hat{\rho}_\beta^{\text{TH}\,0} \equiv \hat{\rho}_\beta^{\text{TH}}[\{a_i^{\beta\,0}\}]$, and

$$\langle \mathcal{S}_{\text{IRR}} \rangle = \beta\big\{\mathcal{F}[\hat{\rho}(\tau)] - \mathcal{F}\big[\hat{\rho}_\beta^{\text{TH}\,\tau}\big]\big\}, \tag{B4}$$

with $\hat{\rho}_\beta^{\text{TH}\,\tau} \equiv \hat{\rho}_\beta^{\text{TH}}[\{a_i^{\beta\,\tau}\}]$.

Then, using Eq (B2), these two expressions can be rewritten as

$$\langle w \rangle = \sum_i \big\{\lambda_i^\tau a_i^\tau - \lambda_i^0 a_i^{\beta\,0}\big\} + \big\{\Omega\big[\big\{a_i^\tau\big\}\big] - \Omega\big[\big\{a_i^{\beta\,0}\big\}\big]\big\} \tag{B5}$$

and

$$\langle \mathcal{S}_{\mathrm{IRR}} \rangle = \beta \sum_i \{\lambda_i^\tau a_i^\tau - \lambda_i^0 a_i^{\beta\, 0}\} - \beta\{\Omega[\{a_i^\tau\}] - \Omega[\{a_i^{\beta\, \tau}\}]\}, \tag{B6}$$

where $\Omega[\{a_i^\tau\}]$ represents the universal part of the out-of-equilibrium free energy. As previously stated, this part is generally unknown, which significantly increases the complexity of the problem. However, suitable approximations can generally be found [45–48], highly dependent on the regimes under consideration, ranging from adiabatic to nearly sudden-quench evolutions. Indeed, in the $\tau \to 0$ limit, Eqs. (B5) and (B6) reduce to the expressions derived in Sec. III B for sudden-quench protocols.

APPENDIX C: DERIVATION OF THE FLUCTUATION-DISSIPATION RELATIONS FOR INFINITESIMAL SUDDEN QUENCHES

We provide here a derivation of Eqs. (28) and (30), yielding the fluctuation-dissipation relations (27) and (31) in the sudden-quench regime. We then consider a sudden-quench protocol starting from a thermal state $\hat{\rho}_\beta^{\mathrm{TH}}$, or more generally for an initial Gibbs state commuting with $\hat{\mathcal{H}}[\{\lambda_i^0\}]$. Given the characteristic function of work (20), it is straightforward to show that the nth moment of the distribution can be written as

$$\langle w^n \rangle = \mathrm{Tr}\{(\hat{\mathcal{H}}[\{\lambda_i^f\}] - \hat{\mathcal{H}}[\{\lambda_i^0\}])^n \hat{\rho}_\beta^{\mathrm{TH}}[\{\lambda_i^0\}]\}. \tag{C1}$$

Specifically, the second moment of the PDW in a system defined by the Hamiltonian (1), where the external work parameters switch instantaneously from $\{\lambda_i\}$ to $\{\lambda_i + \delta\lambda_i\}$, is given by

$$\langle w^2 \rangle = \sum_i \sum_j \delta\lambda_i \delta\lambda_j \mathrm{Tr}\{\hat{A}_i \hat{A}_j \hat{\rho}_\beta^{\mathrm{TH}}[\{\lambda_i^0\}]\}. \tag{C2}$$

At this point, we want to make explicit the dependence on the thermal densities $\{a_i^\beta\}$.

First, we consider the case where $[\hat{\mathcal{H}}[\{\lambda_i^f\}], \hat{\mathcal{H}}[\{\lambda_i^0\}]] = 0$. The HF theorem [see Eq. (8)] ensures that

$$\frac{\partial^2 \mathcal{F}}{\partial\lambda_j \partial\lambda_i} = \frac{\partial a_i^\beta}{\partial\lambda_j} \tag{C3}$$

and

$$\frac{1}{\mathcal{Z}} \frac{\partial \mathcal{Z}}{\partial \lambda_j} = -\beta a_j^\beta. \tag{C4}$$

On the other hand, we have

$$\frac{\partial \hat{\rho}_\beta^{\mathrm{TH}}}{\partial \lambda_j} = -\beta \hat{A}_j \hat{\rho}_\beta^{\mathrm{TH}} - \hat{\rho}_\beta^{\mathrm{TH}} \frac{1}{\mathcal{Z}} \frac{\partial \mathcal{Z}}{\partial \lambda_j} \tag{C5}$$

and

$$\begin{aligned}\frac{\partial^2 \mathcal{F}}{\partial\lambda_j \partial\lambda_i} &= \mathrm{Tr}\left\{\hat{A}_i \frac{\partial \hat{\rho}_\beta^{\mathrm{TH}}}{\partial \lambda_j}\right\} \\ &= -\beta\, \mathrm{Tr}\{\hat{A}_i \hat{A}_j \hat{\rho}_\beta^{\mathrm{TH}}\} - \mathrm{Tr}\{\hat{A}_i \hat{\rho}_\beta^{\mathrm{TH}}\} \frac{1}{\mathcal{Z}} \frac{\partial \mathcal{Z}}{\partial \lambda_j} \\ &= -\beta\, \mathrm{Tr}\{\hat{A}_i \hat{A}_j \hat{\rho}_\beta^{\mathrm{TH}}\} + \beta a_i^\beta a_j^\beta. \end{aligned} \tag{C6}$$

Comparing Eq. (C3) with (C6), we obtain

$$\mathrm{Tr}\{\hat{A}_i \hat{A}_j \hat{\rho}_\beta^{\mathrm{TH}}[\{\lambda_i^0\}]\} = \beta a_i^\beta a_j^\beta - \frac{1}{\beta} \frac{\partial a_i^\beta}{\partial \lambda_j}. \tag{C7}$$

Then, substituting Eq. (C7) into (C2), we get $\langle w^2 \rangle$ as given in Eq. (28).

We now analyze the scenario where the protocol is noncommutative, and the relation (C5) is no longer valid. Here, we rather have

$$\frac{\partial \hat{\rho}_\beta^{\mathrm{TH}}}{\partial \lambda_j} = -\beta \hat{A}_j \hat{\rho}_\beta^{\mathrm{TH}} - \hat{\rho}_\beta^{\mathrm{TH}} \frac{1}{\mathcal{Z}} \frac{\partial \mathcal{Z}}{\partial \lambda_j} + \sum_{n=2}^{\infty} \frac{(-1)^n}{n!} \beta^n \underbrace{[\hat{\mathcal{H}}, [\hat{\mathcal{H}} \dots [\hat{\mathcal{H}}, \hat{A}_j]]]}_{n \text{ times}} \hat{\rho}_\beta^{\mathrm{TH}}. \tag{C8}$$

Therefore, Eq. (28) is corrected by an infinite series of expectation values over the initial thermal state, which are still functionals of the initial thermal densities:

$$\theta^{(n)}[\{a_i^{\beta\, 0}\}] = \mathrm{Tr}\{\hat{A}_i \underbrace{[\hat{\mathcal{H}}, [\hat{\mathcal{H}} \dots [\hat{\mathcal{H}}, \hat{A}_j]]]}_{n \text{ times}} \hat{\rho}_\beta^{\mathrm{TH}}\}. \tag{C9}$$

Consequently, the second moment of the PDW reads as

$$\langle w^2 \rangle = \langle w^2 \rangle_c + \Theta_2[\{a_i^{\beta\, 0}\}], \tag{C10}$$

with

$$\begin{aligned}\Theta_2[\{a_i^{\beta\, 0}\}] &= \sum_{i,j} \delta\lambda_i \delta\lambda_j \sum_{n=2}^{\infty} \frac{(-1)^n}{n!} \beta^{n-1} \\ &\quad \times \mathrm{Tr}\{\hat{A}_i \underbrace{[\hat{\mathcal{H}}, [\hat{\mathcal{H}} \dots [\hat{\mathcal{H}}, \hat{A}_j]]]}_{n \text{ times}} \hat{\rho}_\beta^{\mathrm{TH}}\} \\ &= \sum_i \sum_j \delta\lambda_i \delta\lambda_j \sum_{n=2}^{\infty} \frac{(-1)^n}{n!} \beta^{n-1} \theta^{(n)}[\{a_i^{\beta\, 0}\}]. \end{aligned} \tag{C11}$$

APPENDIX D: HUBBARD MODEL IN A LATTICE WITH ONE SITE

Let us consider the single-site Hubbard model whose Hamiltonian is

$$\hat{\mathcal{H}} = \mathrm{v}_0(\hat{n}_\uparrow + \hat{n}_\downarrow) + U \hat{n}_\uparrow \hat{n}_\downarrow. \tag{D1}$$

Equation (D1) describes a closed system, with an interacting thermal density

$$\begin{aligned} n_\beta &= \mathrm{Tr}\{\hat{n} \hat{\rho}_\beta^{\mathrm{TH}}\} = \mathrm{Tr}\{(\hat{n}_\uparrow + \hat{n}_\downarrow) \hat{\rho}_\beta^{\mathrm{TH}}\} \\ &= \frac{2[e^{-\beta \mathrm{v}_0} + e^{-\beta(2\mathrm{v}_0 + U)}]}{\mathcal{Z}}, \end{aligned} \tag{D2}$$

depending on the canonical partition function

$$\mathcal{Z} = \mathrm{Tr}\{e^{-\beta \hat{\mathcal{H}}}\} = 1 + 2e^{-\beta \mathrm{v}_0} + e^{-\beta(2\mathrm{v}_0 + U)}. \tag{D3}$$

Equation (D2), defining the thermal occupations of the model, depends only on v_0. It can be inverted explicitly to obtain

$$\mathrm{v}_0[n_\beta] = -U - \frac{1}{\beta} \ln \mathcal{G}_U^\beta[n_\beta], \tag{D4}$$

where

$$\mathcal{G}_U^\beta[n_\beta] = \frac{\delta n_\beta + \sqrt{\delta n_\beta^2 + e^{-\beta U}(1-\delta n_\beta)^2}}{1-\delta n_\beta} \tag{D5}$$

and $\delta n_\beta = n_\beta - 1$. With the external potential expressed as a functional of the density, we can also write the partition function as an explicit functional of the density:

$$\mathcal{Z}[n_\beta] = 1 + e^{\beta U}\left(2\mathcal{G}_U^\beta[n_\beta] + \mathcal{G}_U^\beta[n_\beta]^2\right). \tag{D6}$$

Consequently, the noninteracting KS Hamiltonian for the single-site Hubbard model reads as

$$\hat{\mathcal{H}}^{\mathrm{KS}} = V^{\mathrm{KS}}(\hat{n}_\uparrow + \hat{n}_\downarrow) = (\mathrm{v}_0 + V^{\mathrm{H\text{-}XC}})(\hat{n}_\uparrow + \hat{n}_\downarrow). \tag{D7}$$

As it has been done for the interacting single site it is possible to invert the relation

$$n_\beta^{\mathrm{KS}} = \mathrm{Tr}\{\hat{n}\hat{\rho}_{\beta_{\mathrm{KS}}}^{\mathrm{TH}}\} = \frac{2[e^{-\beta V^{\mathrm{KS}}} + e^{-2\beta(V^{\mathrm{KS}})}]}{1 + 2e^{-\beta V^{\mathrm{KS}}} + 2e^{-2\beta V^{\mathrm{KS}}}}, \tag{D8}$$

for the KS thermal density, and obtain

$$V^{\mathrm{KS}}[n_\beta^{\mathrm{KS}}] = -\frac{1}{\beta}\ln\frac{n_\beta^{\mathrm{KS}}}{2 - n_\beta^{\mathrm{KS}}}. \tag{D9}$$

By forcing $n_\beta^{\mathrm{KS}} = n_\beta$, the defining expression of the H-XC potential can be written as

$$V^{\mathrm{H\text{-}XC}}[n_\beta] = U + \frac{1}{\beta}\ln\Gamma_U^\beta[n_\beta], \tag{D10}$$

where

$$\Gamma_U^\beta[n_\beta] = \frac{\delta n_\beta + \sqrt{\delta n_\beta^2 + e^{-\beta U}\left(1 - \delta n_\beta^2\right)}}{n_\beta^{\mathrm{KS}}}. \tag{D11}$$

---

[1] P. Hohenberg and W. Kohn, Inhomogeneous electron gas, Phys. Rev. **136**, B864 (1964).

[2] W. Kohn and L. J. Sham, Self-consistent equations including exchange and correlation effects, Phys. Rev. **140**, A1133 (1965).

[3] E. Runge and E. K. U. Gross, Density-functional theory for time-dependent systems, Phys. Rev. Lett. **52**, 997 (1984).

[4] C. A. Ullrich, *Time-Dependent Density-Functional Theory* (Oxford University Press, Oxford, 2012).

[5] N. D. Mermin, Thermal properties of the inhomogeneous electron gas, Phys. Rev. **137**, A1441 (1965).

[6] K. Burke, J. C. Smith, P. E. Grabowski, and A. Pribram-Jones, Exact conditions on the temperature dependence of density functionals, Phys. Rev. B **93**, 195132 (2016).

[7] A. Pribram-Jones, P. E. Grabowski, and K. Burke, Thermal density functional theory: Time-dependent linear response and approximate functionals from the fluctuation-dissipation theorem, Phys. Rev. Lett. **116**, 233001 (2016).

[8] J. C. Smith, A. Pribram-Jones, and K. Burke, Exact thermal density functional theory for a model system: Correlation components and accuracy of the zero-temperature exchange-correlation approximation, Phys. Rev. B **93**, 245131 (2016).

[9] Z.-H. Yang, J. R. Trail, A. Pribram-Jones, K. Burke, R. J. Needs, and C. A. Ullrich, Exact and approximate Kohn-Sham potentials in ensemble density-functional theory, Phys. Rev. A **90**, 042501 (2014).

[10] S. Pittalis, C. R. Proetto, A. Floris, A. Sanna, C. Bersier, K. Burke, and E. K. U. Gross, Exact conditions in finite temperature density functional theory, Phys. Rev. Lett. **107**, 163001 (2011).

[11] P. Hollebon and T. Sjostrom, Hybrid Kohn-Sham+Thomas-Fermi scheme for high-temperature density functional theory, Phys. Rev. B **105**, 235114 (2022).

[12] A. J. White and L. A. Collins, Fast and universal Kohn-Sham density functional theory algorithm for warm dense matter to hot dense plasma, Phys. Rev. Lett. **125**, 055002 (2020).

[13] S. Kurth and G. Stefanucci, Nonequilibrium Anderson model made simple with density functional theory, Phys. Rev. B **94**, 241103(R) (2016).

[14] V. V. Karasiev, L. Calderín, and S. B. Trickey, Importance of finite-temperature exchange correlation for warm dense matter calculations, Phys. Rev. E **93**, 063207 (2016).

[15] F. Graziani, M. P. Desjarlais, R. Redmer, and S. B. Trickey, *Frontiers and Challenges in Warm Dense Matter* (Springer, Berlin, 2014).

[16] C. Jarzynski, Nonequilibrium equality for free energy differences, Phys. Rev. Lett. **78**, 2690 (1997).

[17] M. Esposito, U. Harbola, and S. Mukamel, Nonequilibrium fluctuations, fluctuation theorems, and counting statistics in quantum systems, Rev. Mod. Phys. **81**, 1665 (2009).

[18] T. B. Batalhão, A. M. Souza, L. Mazzola, R. Auccaise, R. S. Sarthour, I. S. Oliveira, J. Goold, G. De Chiara, M. Paternostro, and R. M. Serra, Experimental reconstruction of work distribution and study of fluctuation relations in a closed quantum system, Phys. Rev. Lett. **113**, 140601 (2014).

[19] T. B. Batalhão, A. M. Souza, R. S. Sarthour, I. S. Oliveira, M. Paternostro, E. Lutz, and R. M. Serra, Irreversibility and the arrow of time in a quenched quantum system, Phys. Rev. Lett. **115**, 190601 (2015).

[20] F. Campaioli, S. Gherardini, J. Q. Quach, M. Polini, and G. M. Andolina, Colloquium: Quantum batteries, Rev. Mod. Phys. **96**, 031001 (2024).

[21] M. Campisi, P. Hänggi, and P. Talkner, Quantum fluctuation relations and the arrow of time, Rev. Mod. Phys. **83**, 771 (2011).

[22] J. Goold, M. Huber, A. Riera, L. Del Rio, and P. Skrzypczyk, The role of quantum information in thermodynamics—a topical review, J. Phys. A: Math. Theor. **49**, 143001 (2016).

[23] J. Klatzow, J. N. Becker, P. M. Ledingham, C. Weinzetl, K. T. Kaczmarek, D. J. Saunders, J. Nunn, I. A. Walmsley, R. Uzdin, and E. Poem, Experimental demonstration of quantum effects in the operation of microscopic heat engines, Phys. Rev. Lett. **122**, 110601 (2019).

[24] M. Perarnau-Llobet, K. V. Hovhannisyan, M. Huber, P. Skrzypczyk, N. Brunner, and A. Acín, Extractable work from correlations, Phys. Rev. X **5**, 041011 (2015).

[25] K. Korzekwa, M. Lostaglio, J. Oppenheim, and D. Jennings, The extraction of work from quantum coherence, New J. Phys. **18**, 023045 (2016).

[26] H.-L. Shi, S. Ding, Q.-K. Wan, X.-H. Wang, and W.-L. Yang, Entanglement, coherence, and extractable work in quantum batteries, Phys. Rev. Lett. **129**, 130602 (2022).

[27] G. Gour, Role of quantum coherence in thermodynamics, PRX Quantum **3**, 040323 (2022).

[28] F. L. Rodrigues and E. Lutz, Nonequilibrium thermodynamics of quantum coherence beyond linear response, Commun. Phys. **7**, 61 (2024).

[29] O. Onishchenko, G. Guarnieri, P. Rosillo-Rodes, D. Pijn, J. Hilder, U. Poschinger, M. Perarnau-Llobet, J. Eisert, and F. Schmidt-Kaler, Probing coherent quantum thermodynamics using a trapped ion, Nat. Commun. **15**, 6974 (2024).

[30] G. Francica, J. Goold, and F. Plastina, Role of coherence in the nonequilibrium thermodynamics of quantum systems, Phys. Rev. E **99**, 042105 (2019).

[31] G. Francica, Class of quasiprobability distributions of work with initial quantum coherence, Phys. Rev. E **105**, 014101 (2022).

[32] A. D. Varizi, A. P. Vieira, C. Cormick, R. C. Drumond, and G. T. Landi, Quantum coherence and criticality in irreversible work, Phys. Rev. Res. **2**, 033279 (2020).

[33] A. D. Varizi, M. A. Cipolla, M. Perarnau-Llobet, R. C. Drumond, and G. T. Landi, Contributions from populations and coherences in non-equilibrium entropy production, New J. Phys. **23**, 063027 (2021).

[34] M. Herrera, J. H. Reina, I. D'Amico, and R. M. Serra, Correlation-boosted quantum engine: A proof-of-principle demonstration, Phys. Rev. Res. **5**, 043104 (2023).

[35] K. Zawadzki, G. A. Canella, V. V. França, and I. D'Amico, Work statistics and entanglement across the fermionic superfluid-insulator transition, Adv. Quantum Technol. **7**, 2300237 (2024).

[36] G. Francica, F. C. Binder, G. Guarnieri, M. T. Mitchison, J. Goold, and F. Plastina, Quantum coherence and ergotropy, Phys. Rev. Lett. **125**, 180603 (2020).

[37] G. Francica, J. Goold, F. Plastina, and M. Paternostro, Daemonic ergotropy: Enhanced work extraction from quantum correlations, npj Quantum Inf. **3**, 12 (2017).

[38] K. Ptaszyński and M. Esposito, Quantum and classical contributions to entropy production in fermionic and bosonic gaussian systems, PRX Quantum **4**, 020353 (2023).

[39] K. T. Geier and P. Hauke, From non-hermitian linear response to dynamical correlations and fluctuation-dissipation relations in quantum many-body systems, PRX Quantum **3**, 030308 (2022).

[40] D. Hahn, M. Dupont, M. Schmitt, D. J. Luitz, and M. Bukov, Quantum many-body Jarzynski equality and dissipative noise on a digital quantum computer, Phys. Rev. X **13**, 041023 (2023).

[41] J.-W. Zhang, B. Wang, W.-F. Yuan, J.-C. Li, J.-T. Bu, G.-Y. Ding, W.-Q. Ding, L. Chen, F. Zhou, and M. Feng, Energy-conversion device using a quantum engine with the work medium of two-atom entanglement, Phys. Rev. Lett. **132**, 180401 (2024).

[42] É. Jussiau, L. Bresque, A. Auffèves, K. W. Murch, and A. N. Jordan, Many-body quantum vacuum fluctuation engines, Phys. Rev. Res. **5**, 033122 (2023).

[43] J. Jaramillo, M. Beau, and A. del Campo, Quantum supremacy of many-particle thermal machines, New J. Phys. **18**, 075019 (2016).

[44] T. Denzler and E. Lutz, Efficiency fluctuations of a quantum heat engine, Phys. Rev. Res. **2**, 032062(R) (2020).

[45] K. Zawadzki, A. H. Skelt, and I. D'Amico, Approximating quantum thermodynamic properties using DFT, J. Phys.: Condens. Matter **34**, 274002 (2022)

[46] A. H. Skelt, K. Zawadzki, and I. D'Amico, Many-body effects on the thermodynamics of closed quantum systems, J. Phys. A: Math. Theor. **52**, 485304 (2019).

[47] M. Herrera, K. Zawadzki, and I. D'Amico, Melting a Hubbard dimer: benchmarks of 'ALDA' for quantum thermodynamics, Eur. Phys. J. B **91**, 248 (2018).

[48] M. Herrera, R. M. Serra, and I. D'Amico, DFT-inspired methods for quantum thermodynamics, Sci. Rep. **7**, 4655 (2017).

[49] L.-A. Wu, M. S. Sarandy, D. A. Lidar, and L. J. Sham, Linking entanglement and quantum phase transitions via density-functional theory, Phys. Rev. A **74**, 052335 (2006).

[50] K. Schönhammer, O. Gunnarsson, and R. M. Noack, Density-functional theory on a lattice: Comparison with exact numerical results for a model with strongly correlated electrons, Phys. Rev. B **52**, 2504 (1995).

[51] J. Coe, I. D'Amico, and V. França, Uniqueness of density-to-potential mapping for fermionic lattice systems, Europhys. Lett. **110**, 63001 (2015).

[52] M. Penz and R. van Leeuwen, Density-functional theory on graphs, J. Chem. Phys. **155**, 244111 (2021).

[53] L. Xu, J. Mao, X. Gao, and Z. Liu, Extensibility of Hohenberg-Kohn theorem to general quantum systems, Adv. Quantum Technol. **5**, 2200041 (2022).

[54] V. V. França, J. P. Coe, and I. D'Amico, Testing density-functional approximations on a lattice and the applicability of the related Hohenberg-Kohn-like theorem, Sci. Rep. **8**, 664 (2018).

[55] R. M. Dreizler and E. K. Gross, *Density Functional Theory: An Approach to the Quantum Many-body Problem* (Springer, Berlin, 2012).

[56] F. C. Alcaraz and M. S. Sarandy, Finite-size corrections to entanglement in quantum critical systems, Phys. Rev. A **78**, 032319 (2008).

[57] M. Pons, B. Juliá-Díaz, A. Polls, A. Rios, and I. Vidana, The Hellmann–Feynman theorem at finite temperature, Am. J. Phys. **88**, 503 (2020).

[58] G. T. Landi and M. Paternostro, Irreversible entropy production: From classical to quantum, Rev. Mod. Phys. **93**, 035008 (2021).

[59] J. Kurchan, A quantum fluctuation theorem, arXiv:cond-mat/0007360.

[60] H. Tasaki, Jarzynski relations for quantum systems and some applications, arXiv:cond-mat/0009244.

[61] P. Talkner, E. Lutz, and P. Hänggi, Fluctuation theorems: Work is not an observable, Phys. Rev. E **75**, 050102(R) (2007).

[62] A. E. Allahverdyan and T. M. Nieuwenhuizen, Fluctuations of work from quantum subensembles: The case against quantum work-fluctuation theorems, Phys. Rev. E **71**, 066102 (2005).

[63] M. Perarnau-Llobet, E. Bäumer, K. V. Hovhannisyan, M. Huber, and A. Acìn, No-go theorem for the characterization of work fluctuations in coherent quantum systems, Phys. Rev. Lett. **118**, 070601 (2017).

[64] K. V. Hovhannisyan and A. Imparato, Energy conservation and fluctuation theorem are incompatible for quantum work, Quantum **8**, 1336 (2024).

[65] G. Rubino, K. V. Hovhannisyan, P. Skrzypczyk, Revising the quantum work fluctuation framework to encompass energy conservation, arXiv:2406.18632.
[66] G. E. Crooks, Entropy production fluctuation theorem and the nonequilibrium work relation for free energy differences, Phys. Rev. E **60**, 2721 (1999).
[67] S. Deffner and E. Lutz, Generalized Clausius inequality for nonequilibrium quantum processes, Phys. Rev. Lett. **105**, 170402 (2010).
[68] R. Kawai, J. M. R. Parrondo, and C. V. den Broeck, Dissipation: The phase-space perspective, Phys. Rev. Lett. **98**, 080602 (2007).
[69] A. Messiah, *Quantum Mechanics* (Dover, New York, 2014).
[70] R. H. Wood, W. C. Muhlbauer, and P. T. Thompson, Systematic errors in free energy perturbation calculations due to a finite sample of configuration space: Sample-size hysteresis, J. Phys. Chem. **95**, 6670 (1991).
[71] D. Hendrix and C. Jarzynski, A “fast growth” method of computing free energy differences, J. Phys. Chem. **114**, 5974 (2001).
[72] H. J. D. Miller, M. Scandi, J. Anders, and M. Perarnau-Llobet, Work fluctuations in slow processes: Quantum signatures and optimal control, Phys. Rev. Lett. **123**, 230603 (2019).
[73] M. Scandi, H. J. D. Miller, J. Anders, and M. Perarnau-Llobet, Quantum work statistics close to equilibrium, Phys. Rev. Res. **2**, 023377 (2020).
[74] K. Capelle and V. L. Campo, Jr., Density functionals and model Hamiltonians: Pillars of many-particle physics, Phys. Rep. **528**, 91 (2013).
[75] V. V. França and K. Capelle, Entanglement in spatially inhomogeneous many-fermion systems, Phys. Rev. Lett. **100**, 070403 (2008).
[76] A. Görling and M. Levy, Exact Kohn-Sham scheme based on perturbation theory, Phys. Rev. A **50**, 196 (1994).
[77] A. Görling and M. Levy, Correlation-energy functional and its high-density limit obtained from a coupling-constant perturbation expansion, Phys. Rev. B **47**, 13105 (1993).
[78] S. Pratt, Canonical and microcanonical calculations for Fermi systems, Phys. Rev. Lett. **84**, 4255 (2000).
[79] P. Borrmann and G. Franke, Recursion formulas for quantum statistical partition functions, J. Chem. Phys. **98**, 2484 (1993).
[80] J.-C. Pain, F. Gilleron, and Q. Porcherot, Generating functions for canonical systems of fermions, Phys. Rev. E **83**, 067701 (2011).
[81] H. Barghathi, J. Yu, and A. Del Maestro, Theory of noninteracting fermions and bosons in the canonical ensemble, Phys. Rev. Res. **2**, 043206 (2020).
[82] A. Pribram-Jones, S. Pittalis, E. K. U. Gross, and K. Burke, Thermal Density Functional Theory in context, in *Frontiers and Challenges in Warm Dense Matter*, edited by M. Schlanges and H. R. Schmidt (Springer, Berlin, 2014), pp. 25–60.
[83] M. C. Gutzwiller, Effect of correlation on the ferromagnetism of transition metals, Phys. Rev. Lett. **10**, 159 (1963).
[84] J. Hubbard, Electron correlations in narrow energy bands, Proc. R. Soc. London A **276**, 238 (1963).
[85] J. Kanamori, Electron correlation and ferromagnetism of transition metals, Prog. Theor. Phys. **30**, 275 (1963).
[86] S. Murmann, A. Bergschneider, V. M. Klinkhamer, G. Zürn, T. Lompe, and S. Jochim, Two fermions in a double well: Exploring a fundamental building block of the Hubbard model, Phys. Rev. Lett. **114**, 080402 (2015).
[87] Editorial, The Hubbard model at half a century, Nat. Phys. **9**, 523 (2013).
[88] D. Carrascal, J. Ferrer, J. C. Smith, and K. Burke, The Hubbard dimer: A density functional case study of a many-body problem, J. Phys.: Condens. Matter **27**, 393001 (2015).
[89] V. L. Campo, Density-functional-theory approach to the thermodynamics of the harmonically confined one-dimensional Hubbard model, Phys. Rev. A **92**, 013614 (2015).
[90] X. Gao, A.-H. Chen, I. V. Tokatly, and S. Kurth, Lattice density functional theory at finite temperature with strongly density-dependent exchange-correlation potentials, Phys. Rev. B **86**, 235139 (2012).
[91] G. Stefanucci and S. Kurth, Towards a description of the Kondo effect using time-dependent density-functional theory, Phys. Rev. Lett. **107**, 216401 (2011).
[92] I. D’Amico, J. P. Coe, V. V. França, and K. Capelle, Quantum mechanics in metric space: Wave functions and their densities, Phys. Rev. Lett. **106**, 050401 (2011).
[93] A. D. Becke, Density-functional exchange-energy approximation with correct asymptotic behavior, Phys. Rev. A **38**, 3098 (1988).
[94] J. P. Perdew, J. A. Chevary, S. H. Vosko, K. A. Jackson, M. R. Pederson, D. J. Singh, and C. Fiolhais, Atoms, molecules, solids, and surfaces: Applications of the generalized gradient approximation for exchange and correlation, Phys. Rev. B **46**, 6671 (1992).
[95] J. P. Perdew, K. Burke, and M. Ernzerhof, Generalized gradient approximation made simple, Phys. Rev. Lett. **77**, 3865 (1996).
[96] M. Levy, Universal variational functionals of electron densities, first-order density matrices, and natural spin-orbitals and solution of the v-representability problem, Proc. Natl. Acad. Sci. USA **76**, 6062 (1979).
[97] T.-c. Li and P.-q. Tong, Hohenberg-Kohn theorem for time-dependent ensembles, Phys. Rev. A **31**, 1950 (1985).
[98] I. V. Tokatly, Time-dependent current density functional theory on a lattice, Phys. Rev. B **83**, 035127 (2011).
[99] C. Verdozzi, Time-dependent density-functional theory and strongly correlated systems: Insight from numerical studies, Phys. Rev. Lett. **101**, 166401 (2008).